# Collaboration as a Key to Advance Capabilities for Earth-abundant Metal Catalysis

Paul J. Chirika, Keary M. Engleb, Eric M. Simmonsc\* and Steven R. Wisniewskic\*

- \*Email: eric.simmons@bms.com, steven.wisniewski@bms.com
- <sup>a</sup> Department of Chemistry, Princeton University, Princeton, New Jersey 08544, United States
- <sup>b</sup> Department of Chemistry, Scripps Research, La Jolla, California 92037, United States
- <sup>c</sup> Chemical Process Development, Bristol Myers Squibb Company, New Brunswick, New Jersey 08903, United States

#### **Abstract**

Earth-abundant metal (EAM) catalysis can have profound impact in the pharmaceutical industry in terms of sustainability and cost improvements from replacing precious metals like palladium, as well as harnessing the differential reactivity of first-row metals that allows for novel transformations to enable more efficient routes to clinical candidates. The strategy for building these capabilities within the process group at Bristol Myers Squibb is described herein, with the general plan of building a reaction screening platform, demonstrating scalability, and increasing mechanistic understanding of the reaction and catalyst activation. The development of catalytic transformations utilizing nickel, cobalt, and iron is described while highlighting the importance of collaboration with internal and external groups to advance EAM catalysis and impact our portfolio. The challenges and benefits of working with first-row transition metals, including metrics for the implementation of EAM catalysis, such as cost, process mass intensity (PMI), commercial availability of catalysts and ligands, are discussed.

**Keywords:** earth abundant metal catalysis, base metal catalysis, cross coupling, nickel, cobalt, iron, sustainability

#### Introduction

The importance of transition metals in the synthesis of modern pharmaceutically relevant compounds is difficult to overstate. Wey bond formations made possible by transition metal catalysis enable synthetic disconnections that would otherwise be difficult or impossible, often leading to shorter, more efficient and ideally more sustainable syntheses of drug candidates and pharmaceutical products. These transformations are routinely used in medicinal chemistry, including parallel library synthesis, and have been applied extensively on large scale, including commercial manufacturing routes for approved drugs. While the chemical processes mediated by transition metals and their associated substrate pools will undoubtedly continue to evolve and expand, the continued central role of catalysis in the discovery, development and large-scale synthesis of drug candidates and marketed medicines seems all but certain.

Given the importance of transition metal-catalyzed processes in the development of routes to drug candidates, the process department at Bristol Myers Squibb (BMS) has a dedicated catalysis group to accelerate and enhance applications of catalysis across the portfolio, which has been operating continuously for nearly 15 years. During this time, the group has collaborated extensively with colleagues in both the process development and discovery chemistry organizations, leveraging state of the art tools and techniques, such as automation and high-throughput experimentation (HTE),9 to investigate a diverse array of metal-catalyzed transformations to enable the advancement of our pipeline. A retrospective analysis of the individual reactions studied by the group over this time period reveals that the most heavily utilized transformations are C-C cross-coupling (predominantly Pd-catalyzed Suzuki-Miyaura couplings<sup>10</sup> of arylboronic acids and esters), C-N coupling (predominantly Buchwald-Hartwig couplings with Pd catalysts<sup>11</sup>) and borylation (predominantly Pd-catalyzed Miyaura borylation of aryl halides with diboron reagents<sup>12</sup>). For each of these reaction types, >50 unique substrates from our internal portfolio have been investigated in detail, and dozens of developed process have been executed on multi-kilogram scale. 13 It is important to emphasize both the prevalence of borylation reactions and the dominance of Suzuki-Miyaura coupling (SMC) relative to other C-C cross-coupling technologies. These interrelated trends are a result of the stability and wide commercial availability of neutral organoboron coupling partners, as well as the mild reaction conditions for SMC that lead to high functional group tolerance, 14 all of which are highly attractive features for applications in complex molecule synthesis. It should also be noted that the preference for SMC over other cross-coupling technologies for C-C bond formation appears to be quite general across the pharmaceutical industry. 6,9c

As the capabilities and knowledge base of our catalysis group has matured, we have become increasingly interested in building our understanding of Earth-abundant metals (EAMs) and evaluating their potential to impact our portfolio. In this Perspective, we discuss recent and ongoing efforts to complement our existing capabilities for the discovery and implementation of precious metal-catalyzed processes (typically utilizing Pd catalysts) with technologies that enable the development of transformations catalyzed by EAMs, namely Ni, Co and Fe. In line with the drivers noted about heavily favoring the use of neutral organoboron coupling partners, much of our efforts with EAMs have focused on methods that generate these species as products or utilize them as reactants under mild conditions. A central theme that will be highlighted throughout the manuscript is the establishment of highly productive collaborations—both internal to BMS and with external academic collaborators—that have been essential to our efforts to build capabilities in EAM catalysis. Specifically, as a complement to the dedicated catalysis group at BMS, we recently began operating a broader catalysis community of practice (our Catalysis CoP) to facilitate the sharing of knowledge related to the development of catalytic processes, to democratize research efforts, and to expand our collective catalysis capabilities. In addition, we have established highly productive collaborations with two leading academic research groups in the field of EAM catalysis, Prof. Keary Engle's group at the Scripps Research Institute and Prof. Paul Chirik's group at Princeton University. Finally, though BMS is not a participating company, we would like to acknowledge the impactful collaborative work that is

being done by the precompetitive alliance for nonprecious metal catalysis at AbbVie, Boehringer Ingelheim and Pfizer,<sup>15</sup> which has led to a number of advances in the field of EAM catalysis and has inspired and influenced many of our own efforts in this area.

Motivations. Several recent reviews discuss the opportunities and challenges for developing catalytic transformations using Earth-abundant first-row metals, 16 which we will accordingly mention here only briefly. On one hand, the significantly higher terrestrial abundance<sup>17</sup> and lower cost (from both a financial and environmental standpoint) of Earth-abundant first-row metals compared to late second- and third-row precious metals is a key factor motivating research to replace precious metal catalysts with EAMs. As an example, the cost (on a per mol basis) of Ni is nearly three orders of magnitude lower than Pd, with a similar difference in the estimated global warming potential (GWP) for the production of 1 kg of Ni compared to 1 kg of Pd (6.5 vs. 3,880 kg equivalents of CO<sub>2</sub>). 18,19 It has also been noted that the ligands that enable productive catalysis with EAMs, such as Ni, are in many cases simpler and less expensive than those involved in Pd-catalyzed process, which in some cases can be a critical factor impacting both the cost and sustainability of a chemical process.<sup>20</sup> A complementary and equally important driver for EAM catalysis is the unique properties of EAMs that enable them to catalyze transformations that are challenging for precious metals, such as the activation of less reactive C-O bonds,<sup>21</sup> cross-couplings involving C(sp<sup>3</sup>)hybridized coupling partners8 or entirely new reaction manifolds, such as metallaphotoredox catalysis22 and the combination of transition metal catalysis with electrochemistry.<sup>23,24</sup> As will be highlighted in more detail, these features of EAM catalysis have the potential to impact route invention by enabling new disconnections and through an expanded pool of starting materials.

Toxicity and safety. A detailed discussion of metal toxicity is beyond the scope of this Perspective, and we instead direct the reader to a series of publications by Ananikov and coworkers that compare the toxicity of various Earth-abundant and precious metals. <sup>25</sup> In brief, it has been noted that the toxicity of a metal depends on a number of factors, including route of exposure, oxidation state, particle size, and coordination sphere that in turn influence solubility, bioavailability and cellular transport pathways, thereby complicating any attempts at a generalized comparison of the toxicity of Earth-abundant and precious metals. <sup>25a</sup> In the context of the synthesis of pharmaceutically relevant molecules, the International Council for Harmonisation of Technical Requirements for Pharmaceuticals for Human Use (ICH) guidelines for elemental impurities establishes limits for the amount of residual metal in active pharmaceutical ingredients (APIs). While the permitted daily exposure (PDE) for each element depends on the route of administration and dosage, for oral drugs with daily doses of <10 g per day, the permissible levels of catalytically-relevant transition metals range from 5 ppm for Co to 300 ppm for Cu (Table 1); notably, there are currently no specified limits for either Fe or Mn.

Table 1. Permitted daily exposure (PDE) for selected elemental impurities according to ICH guidelines.

		Oral		Parenteral		Inhalation	
		PDE	Dose-adjusted	PDE	Dose-adjusted	PDE	Dose-adjusted
Element	Class	μg/day	ppm	μg/day	ppm	μg/day	ppm
Со	2A	50	5	5	0.5	3	0.3
Ni	2A	200	20	20	2	5	0.5
Pd	2B	100	10	10	1	1	0.1
Cu	3	3000	300	300	30	30	3

No PDE limits:

Fe, Mn

It has been suggested that a possible complication of implementing nickel-catalyzed processes on large scale is that nickel(II) chloride, nickel(II) nitrate and other nickel(II) salts, as well as various nickel(0) species such as Ni(cod)<sub>2</sub>, are classified as restricted substances under the REACH<sup>27</sup> regulations of the European Union (EU) and European Chemicals Agency (ECHA). As a result, certain uses for substances on this list are restricted in the EU, which could potentially limit the applications of nickel catalysis in an industrial setting in Europe. However, at present the restricted uses for nickel are exclusively associated with piercings and other articles that come into direct and prolonged contact with exposed skin.<sup>28</sup> Similarly, while several cobalt salts, including cobalt(II) chloride, cobalt(II) nitrate and cobalt(II) acetate have been recommended for inclusion in the REACH Authorisation List,<sup>29</sup> there are currently no restricted uses for these species. While worker safety should never be compromised, all of these salts are non-volatile and can be safely handled using appropriate engineering controls and personal protective equipment (PPE). On the other hand, the vast amount of CO<sub>2</sub> emissions associated with the mining of precious metals, such as Pd,<sup>18</sup> pose a significant threat to the entire planet, including global human health, that cannot be easily mitigated in a similar manner.

*Metal remediation.* As a result of the prevalence of Pd-catalyzed transformations in modern pharmaceutical synthesis, various methods have been developed to aid in its removal from reaction streams in order to meet the strict limits for residual Pd content in APIs (see Table 1),<sup>30</sup> sometimes involving expensive scavengers or resins. Unfortunately, reliance on these technologies for metal remediation generally increases process complexity and cost. In contrast, while more thorough studies are needed, there are encouraging reports in the literature suggesting that residual Ni can, in many cases, be removed from process steams by simple aqueous washes.<sup>31</sup> Thus, there is the potential for EAM catalysis to minimize both the financial and processing burdens for metal removal following reaction completion.

#### Earth-abundant metals as replacement for Pd

*Ni-catalyzed borylation.* The first step in our quest to build EAM capabilities at BMS was to define the philosophy on how we would implement this initiative within our process chemistry group. Our goal was to

develop reaction platforms that could be leveraged to evaluate transformations utilizing EAMs relevant to our current and future portfolio. We saw the evolution of development as follows: 1) strategic selection of the transformation, 2) development of a screening platform, 3) mechanistic investigations to support scalability and robustness, and 4) application to our portfolio. This workflow for constructing our overall program has been successful in building foundational knowledge of the transformations and allowing us to quickly evaluate the feasibility of any transformation of interest with EAMs. It should be noted that the latter three activities are interconnected, and we envisioned that work toward different aims would often be conducted in parallel.

As mentioned previously, the three main types of transition-metal catalyzed transformations developed in our process chemistry group since 2012 are: C-C cross-coupling, C-N cross-coupling, and C-X borylation reactions. Therefore, we decided that it would be most practically useful to build capabilities for one of these three transformations first, as we knew these reaction types would continue to be a vital part of our portfolio. Accordingly, the decision was made to pursue nickel-catalyzed borylation reactions as an entry point to EAM catalysis. We chose to start with nickel as we thought it would be most similar to palladium in terms of its general reactivity in a given transformation and the similarity of ligands and metal precursors for the transformation.<sup>32</sup> The borylation reaction entailed catalyst systems that seemed unlikely to proceed through odd-electron chemistry, further drawing parallels to palladium catalysis. The borylation reaction itself fixes one of the coupling partners as the diboron reagent, limiting the amount of potential variability in the early stages of development. There is also only a narrow pool of diboron coupling partners for this transformation, and we believed that the learnings from one diboron reagent would help inform development of the others. Although there are not many examples of utilizing nickel on scale for borylation reactions, 31a a recently published methodology from Molander showed broad scope of substrates under mild reaction conditions,<sup>33</sup> which we thought could potentially translate to complex pharmaceutically relevant intermediates.

Our initial ventures into EAM catalysis centered on a key project in our portfolio, the development of an inhibitor to Bruton's Tyrosine Kinase (BTK).<sup>34</sup> At that time, the program was projected to need metric tons of BMS-986142 (Scheme 1, left) to support clinical trials and future commercialization, meaning the utilization of an EAM could have immediate cost-savings impact on our portfolio. The installation of the bottom arene ring was achieved through an asymmetric SMC reaction,<sup>34b</sup> where the corresponding boronic acid was prepared utilizing palladium catalysis (Scheme 1, top right). These conditions had been scaled to prepare over 200 kg of the boronic acid, and therefore this borylation reaction was chosen for our foray into nickel-catalyzed borylation reactions.

Scheme 1. Structure of BTK Inhibitor BMS-986142 (left) and Borylation to Key Intermediate (right)

During this initial phase of reaction exploration, we decided to focus on developing a borylation reaction that would be robust, scalable, and economically feasible (i.e., commercially available ligands, catalysts, and reagents). After determining the viability of nickel as a catalyst for the borylation reaction, we sought to understand the impact of the source of nickel precatalyst on the reaction. We made the strategic decision that our initiative would focus on the utilization of inexpensive and readily available nickel(II) salts as precatalysts, such as NiCl<sub>2</sub>•6H<sub>2</sub>O and Ni(NO<sub>3</sub>)<sub>2</sub>•6H<sub>2</sub>O. With these precatalysts, the impact of solvent, ligand, and base on the transformation was investigated. The results of the optimization led to a set of reaction conditions that afforded the desired boronic acid in 96 liquid chromatography area% (LCAP, 220 nm) at the end of the reaction, with the desired product isolated in 80% yield utilizing 0.5 mol % of Ni(NO<sub>3</sub>)<sub>2</sub>•6H<sub>2</sub>O as the precatalyst (Scheme 1, bottom right).<sup>35</sup> If the program had moved forward, the implementation of this nickel-catalyzed borylation would have led to a more sustainable process and an estimated cost savings of \$12 million per year.<sup>36</sup>

With the success of this reaction for the BTK substrate, we wanted to better understand the impact of reaction variables across an array of substrates. We evaluated a panel of both portfolio relevant and commercially available aryl (pseudo)halides using HTE and analyzed the results across this large data set to identify a collection of ligands that were most likely to yield the product. This curated pool of ligands served as our screening platform for evaluating newly encountered substrates for nickel-catalyzed borylations. This screening platform can be rapidly employed to determine the viability of a nickel-catalyzed borylation. If a substrate does not perform well in this screening platform, it will be a very challenging substrate for nickel. We have continued to refine this screening platform based on our learnings since the initial publication, and the screening conditions shown here reflect the platform that we are currently employing to evaluate nickel-catalyzed borylations (Figure 1). Having developed the screening platform, we started to think about other experimental data that would help build confidence in the robustness of nickel-catalyzed borylations. Therefore, we performed a series of experiments to evaluate the stability of tetrahydroxydiboron under an array of conditions (with various solvents, bases, and nickel sources) to understand the ideal order of addition for this transformation, which we learned was addition of the base

last. Further, we sought to understand the remediation of nickel and found that in most cases a large amount of nickel (up to 95%, from a concentration of 1800 ppm with no wash to <80 ppm) could be removed through a single aqueous wash, with a second aqueous wash further reducing residual nickel to <10 ppm.<sup>35</sup>

Ligands (12):				
Cy-JohnPhos	CPhos	PPh <sub>2</sub> Cy		
MePhos	CX-POMeCy	$PPh_3$		
Cy-DavePhos	CX-PCy	$P(p-F-C_6H_4)_3$		
Ph-DavePhos	PCy <sub>3</sub> HBF <sub>4</sub>	$P(p-OMe-C_6H_4)_3$		

Figure 1. Screening platform for nickel-catalyzed borylations.

The ability to rapidly identify and develop conditions for nickel-catalyzed borylation enabled the scalable synthesis of a radiolabeling precursor for the <sup>18</sup>F-analog of our IDO1 inhibitor linrodostat (BMS-986205),<sup>37</sup> which entered phase III clinical trials for the treatment of bladder cancer.<sup>38</sup> Aryl pinacolboronate 1a (Scheme 2) was initially synthesized in milligram quantities by palladium-catalyzed borylation of heteroaryl iodide 2, which in turn was prepared through a ten-step sequence that included a late-stage SFC resolution of four stereoisomers. With a deadline of three months to deliver material to the clinic, we could not utilize this route because the requisite heteroaryl iodide was not available in sufficient quantities, and the synthesis of additional material could not be completed in time. Therefore, we sought to prepare boronate ester 1a from readily available aryl fluoride 3, the final isolated intermediate in the commercial linrodostat process.39 Taking inspiration from a previous report from the Martin group on the borylation of aryl fluorides, 40 we leveraged our internal knowledge on nickel-catalyzed borylations to develop reaction conditions that were scaled to 100 g to effect the borylation of the penultimate compound in the route to linrodostat in 71 area% (HPLC area). The intermediate boronic acid (1b) was purified by prep-LC, followed by condensation with pinacol and subsequent amide bond coupling to afford >20 g of the desired pinacol ester 1a. This material was then transferred to our radiolabeling group, who converted it to the <sup>18</sup>F-labeled linrodostat<sup>41</sup> (Scheme 3) for imaging studies in mice, monkeys and humans. 42 Notably, while the initial focus for our screening platform was to enable the substitution of palladium with nickel for Miyaura borylation of aryl (pseudo)halides, aryl fluorides represent a substrate class that is unreactive with palladium catalysis.

Scheme 2. Comparison of Borylation Conditions for [18F]-Linrodostat Precursor

Scheme 3. Generation of Radiolabeled Linrodostat

This screening platform has been applied to investigate the nickel-catalyzed borylation of every relevant substrate in our portfolio since its inception in 2018, and there are several on-going portfolio projects that utilize a nickel-catalyzed borylation that we look forward to sharing in the near future. For one such program, a second-generation route that implements a nickel-catalyzed borylation of an aryl sulfamate afforded the desired boronate ester in 85% yield on 22 kg scale (eq 1) and has led to a 45% reduction in raw material costs through use of the phenol precursor to the aryl sulfamate as the starting material. Sulfamates are intriguing substrates for nickel-catalyzed borylations as they are stable to many different reaction conditions and unreactive in other types of transition metal catalysis, including under palladium-catalyzed borylation conditions. Thus, as with the aryl fluoride borylation discussed above, this application of nickel-catalyzed borylation is another example where the novel properties and reactivity of nickel can be harnessed to achieve a transformation that is beyond the reach of palladium. The manuscripts describing the development of this route and process are in preparation.

We have amassed data from over 1600 reactions from the optimization and investigation of nickel-catalyzed borylation reactions. With this large data set, we sought to utilize machine learning to further our understanding of this transformation and also shed light on future directions. We first wanted to determine if we could identify trends in the data based on ligand. Interestingly, analysis of top ligands and their average yield are: Cy-JohnPhos (62%),  $P(p-F-C_6H_4)_3$  (61%),  $PPh_2Cy$  (60%). While Cy-JohnPhos (Figure 2) was the top ligand for the several borylations (see above), we learned we should include these other two ligands in initial screening to see how effective they are in a given transformation. Though all three ligands are readily available in bulk quantities, there are potentially significant cost savings from testing these other two ligands. (The three ligands cost \$1.1/mmol, \$0.75/mmol, and \$0.32/mmol, respectively). It is worth noting that the lack of intellectual property (IP) around simple ligands that have been studied for decades, such as  $P(p-F-C_6H_4)_3$  and  $PPh_2Cy$ , is also an advantage as it obviates any licensing considerations and provides freedom to operate for processes that are developed using these ligands. However, more recently developed ligands and (pre)catalysts for EAM catalysis do not always enjoy this advantage as a result of an increasing trend to patent more readily, which can complicate their use on scale.

**Figure 2**. Biaryl monophosphine ligands investigated for nickel-catalyzed borylation using machine learning.

Having identified effective ligands, we wanted to understand what attributes of the ligand were important for reactivity. Modeling of the yields versus ligand descriptors from the *kraken* database<sup>44</sup> showed that highest yields were obtained for ligands with nbo\_bds\_e\_avg\_boltz >0.205 and vbur\_qvbur\_max\_min <16.5 and for quadrant representing nbo\_bds\_e\_avg\_boltz >0.205 and Pint\_P\_max\_boltz >32. These values can be confirmed as including top performing ligands: Cy-JohnPhos, P(*p*-F-C<sub>6</sub>H<sub>4</sub>)<sub>3</sub>, PPh<sub>2</sub>Cy, P(*p*-Anis)<sub>3</sub>, and CX-PCy. These parameters also identify new ligands that could perform well within this space: CPhos, S-Phos, RuPhos, CM-Phos, PPh<sub>2</sub>tBu, PPhCy<sub>2</sub>, and PPh<sub>2</sub>(*o*-Anis).<sup>43</sup> We are currently following up on these ligands to determine if they are suitable ligands for nickel-catalyzed borylations.

In addition to understanding the factors that impact ligand performance, models were built to predict the conversion based on substrate and ligand. The models based on substrate were evaluated against hold-out aryl (pseudo)halides. (Hetero)aryl sulfamates performed poorest in these models, presumably due to the majority of data in the model coming from halide substrates, whereas aryl chlorides performed reasonably well against actual yields. The predictions based on ligand utilized a proximity-based ligand space guided search with eight ligands expected to perform well and four expected to perform poorly. The results of this model were as expected, with PBn<sub>3</sub> and PEt<sub>3</sub> performing worst and P(p-CF<sub>3</sub>-C<sub>6</sub>H<sub>4</sub>)<sub>3</sub>, CX-POMeCy, CX-PInCy, and CM-Phos as the top-performing ligands.<sup>43</sup> We are continuing to evaluate and refine these models as we collect data on the nickel-catalyzed borylation of new substrates.

In defining our strategy for building knowledge around the most heavily utilized transition metal-catalyzed transformations, we have successfully built a screening platform for nickel-catalyzed borylations that can be easily implemented to test a new substrate of interest. To gain knowledge around robustness and scalability, we needed to understand catalyst activation to ensure that we will have a productive catalyst when we are running a borylation on kilogram scale. Initial studies on the binding of phosphine ligands to NiX<sub>2</sub> salts in methanol showed that coordination does not occur. Alternatively, the addition of methanol and DIPEA to NiCl<sub>2</sub>•6H<sub>2</sub>O led to the formation of [Ni(OMe)<sub>2</sub>]<sub>n</sub> as a coordination polymer in reaction solvent (eq 2). The coordination polymer is not soluble in common organic solvents and is not catalytically active, which could cause significant issues on scale by introducing a catalyst deactivation pathway.

NiCl<sub>2</sub>•6H<sub>2</sub>O DIPEA (2 or 19 equiv)
$$\longrightarrow [Ni(OMe)_2]_n$$
MeOH, 23 °C, 2 h
92% yield (2)

The stoichiometric reduction of Ni(II) salts with diboron reagents was next investigated. The addition of increasing equivalents of  $B_2(neo)_2$  in the presence of DIPEA/MeOH led to increased formation of Ni(0) metal, with 8 equiv of  $B_2(neo)_2$  giving >99% yield of Ni black. In a catalytic reaction, the diboron species is present in significantly higher excess relative to nickel so complete precatalyst reduction should be rapid and efficient. The diboron-mediated reduction of nickel(II) parallels our prior learnings of the catalyst

activation of a palladium-catalyzed borylation from our JAK2 program, which showed that catalyst activation could also be mediated by the diboron reagent.<sup>47</sup> To demonstrate that the reduction of Ni(II) salts with diboron reagents can also result in Ni species that could be catalytically active and do not plate out as Ni black, we trapped the Ni(0) species that forms with a wide variety of ligands. One example shows that the addition of triphenylphosphine leads to formation of tetrakis(triphenylphosphine) nickel(0) in 75% yield (Figure 3).<sup>45</sup>

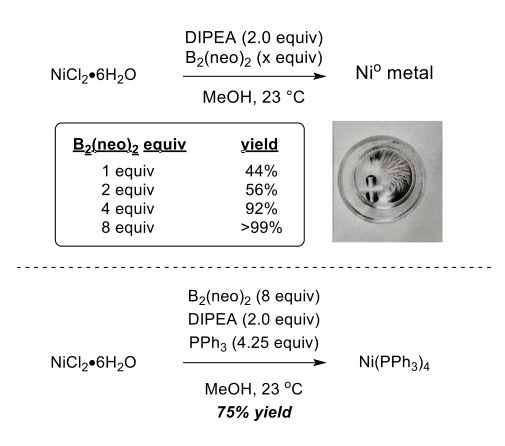


Figure 3. Reduction of Ni(II) with  $B_2(neo)_2$ .

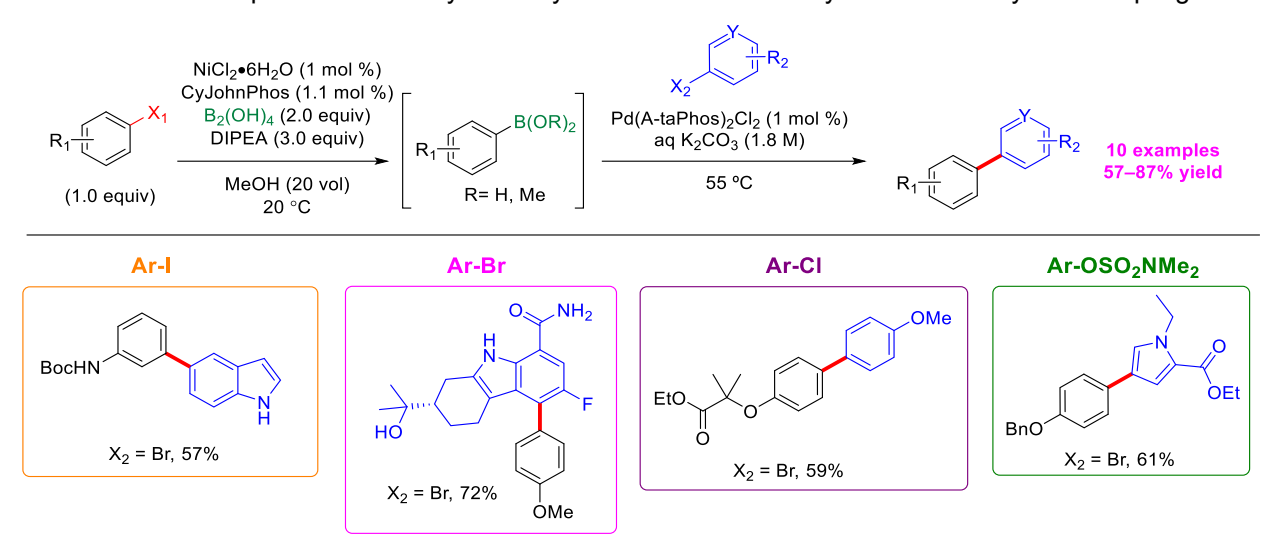
The understanding of catalyst activation, coupled to the screening platform and application to our portfolio completes the platform for development that we established. Therefore, we wanted to compare metrics between a palladium- and nickel-catalyzed borylation, using the BTK aryl bromide as a representative substrate (Table 2). In addition to the improvements in sustainability by utilizing nickel in place of palladium, there are drastic improvements to the cost relative to the metal, ligand and diboron reagent. Most notably, replacing palladium with nickel effectively eliminates any appreciable cost contribution from the metal. Even at a catalyst loading of 1 mol % Pd there is still a significant cost difference between the two processes, with the palladium process being >2.5x the cost of the nickel process. When decreasing to 0.1 mol % loading with Pd, the largest contributor to overall cost becomes the diboron reagent. While the largest impact to cost for the nickel-catalyzed process is also the diboron reagent, this transition occurs at a significantly higher catalyst loading. This model assessment reinforces our belief that we should develop robust chemistry with the lowest catalyst loading tolerable to have the largest impact to cost and sustainability.

Table 2. Cost comparison for Pd and Ni-catalyzed borylation processes for BTK Inhibitor BMS-986142.

	Pd(OAc) <sub>2</sub> Process			NiCl <sub>2</sub> •6H <sub>2</sub> O Process
Metal Loading	2 mol %	1 mol %	0.1 mol %	0.5 mol %
Cost/kg of Boronic Acid	\$784	\$392	\$39	\$0.53
Ligand Loading	4 mol %	2 mol %	0.2 mol %	1 mol %
Cost/kg of Boronic Acid	\$138	\$70	\$7	\$56
Diboron Loading	1.5 equiv	1.5 equiv	1.5 equiv	1.2 equiv
Cost/kg of Boronic Acid	\$271	\$271	\$271	\$216
Total cost from Metal/Ligand/Diboron per kg of Boronic Acid	\$1,193	\$733	\$317	\$273

Telescoped Ni-catalyzed borylation/Pd-catalyzed C(sp<sup>2</sup>) – C(sp<sup>2</sup>) Suzuki–Miyaura coupling. Since the first demonstration of a nickel-catalyzed borylation on our BTK program, we have developed a screening platform, built mechanistic understanding around catalysis robustness, and executed the borylation on kilogram scale within our portfolio. We next looked to build upon this foundation by developing a telescoped nickel-catalyzed borylation/palladium-catalyzed SMC process. As the (hetero)arylboron species is rarely the desired product, implementing a telescoped process has significant advantages in terms of yield, cycle time, and sustainability. Furthermore, in most cases the impurities observed in a borylation reaction are similar to those in a SMC reaction. Molander has previously demonstrated a telescoped palladiumcatalyzed borylation/palladium-catalyzed SMC process, 48 and this sequence has been applied on multikilogram scale at BMS for the synthesis of an LPA-1 antagonist.<sup>49</sup> Percec has demonstrated a nickelcatalyzed borylation of aryl halides with in situ generated neopentylglycol borane followed by a palladiumcatalyzed SMC, but this required the borylation stream to be concentrated to dryness,50 which is not practical on process scale. In collaboration with the Frantz group at The University of Texas at San Antonio (UTSA), we developed a nickel-catalyzed borylation/palladium-catalyzed SMC reaction sequence that does not require an intermediate workup operation. Utilizing Cy-JohnPhos as a ligand for the nickel-catalyzed borylation, addition of aqueous base followed by the subsequent (hetero)aryl halide and Pd(A-taPhos)<sub>2</sub>Cl<sub>2</sub> led to the synthesis of a library of biaryl compounds starting from aryl iodides, chlorides, bromides, and sulfamates (Scheme 4).51 Moreover, we have developed and scaled a nickel-catalyzed borylation/palladium-catalyzed SMC process within the current BMS portfolio. Optimizing on HTE scale at 10 μmol, followed by development at 5 g, demonstration at 50 g, and execution at 1.7 kg, we demonstrated that the same yield, purity, potency, and metal remediation could be achieved for this transformation across scales. We look forward to sharing the full details of the development of this telescoped process in due course.

Scheme 4. Telescoped Nickel-Catalyzed Borylation/Palladium-Catalyzed Suzuki-Miyaura Coupling



The further development of this telescoped process is the next step in our continued evolution of utilizing nickel in Miyaura borylation reactions. As noted previously, there are significant advantages of utilizing nickel in terms of sustainability and cost; however, several challenges remain. One important point to note is that all borylation reactions generate hydrogen gas from the decomposition of the diboron reagent in protic solvents, regardless of the identity of the metal catalyst used.<sup>52</sup> The process group at Eli Lilly recently published an article detailing this hydrogen generation in a palladium-catalyzed borylation/palladium-catalyzed SMC telescope sequence.<sup>53</sup> Therefore, care should be taken when conducting these reactions, as hydrogen can accumulate quickly and build pressure if the reaction is performed in a sealed system. Another challenge that remains is substrate scope. Several types of substrates are generally problematic for nickel catalysis, including those with di-*ortho*-substitution, which are generally unreactive, and polyhalogenated arenes, where chemoselectivity is often poor.<sup>54</sup> We will continue to try to improve conversion and selectivity for these challenging substrates; however, palladium will also play an important role in the continued development and scale-up of borylation reactions in process chemistry, as its reactivity complements that of nickel.

*Ni-catalyzed C(sp²)–C(sp²) Suzuki–Miyaura coupling.* With our work on nickel-catalyzed borylation serving as a foundation, we next sought to build our capabilities and understanding of nickel-catalyzed C(sp²)–C(sp²) SMC. These investigations built upon several decades of key advances in this area, dating back to seminal studies in the late 1990's from Percec,<sup>55</sup> Kobayashi,<sup>56</sup> Miyaura<sup>57</sup> and Indolese.<sup>58</sup> While early works employed exogenous reductants such as  $Zn^{55}$  or n-BuLi<sup>57</sup> to reduce a Ni(II) precatalyst in situ to an active Ni(0) catalyst, later studies demonstrated that Ni(II) precatalysts could be reduced directly under the reaction conditions,<sup>58-59</sup> presumably via double transmetallation of the arylboron coupling partner. However, despite key advancements in the past decade, high catalyst loadings (5–10 mol %) and a large excess of the arylboron coupling partner are frequently required for high yields.<sup>60</sup> Notably, a common limitation of nearly all prior art was the use of inorganic bases with poor solubility in organic solvents, such as  $K_3PO_4$ 

and K<sub>2</sub>CO<sub>3</sub>, often in conjunction with small yet highly specific amounts of water that is either intentionally added or adventitiously present in the inorganic base.<sup>59,61</sup> From the standpoint of reproducibility, robustness and scalability, each of these features were significant drawbacks that we sought to overcome. We considered that the ideal solution would involve the identification of a modular, air-stable precatalyst that readily undergoes activation and promotes cross-coupling at low catalyst loadings using a soluble base with tolerance for a wide range of water levels<sup>62</sup> (Figure 4).

**Figure 4**. Limitations and design goals for Ni-catalyzed C(sp<sup>2</sup>)–C(sp<sup>2</sup>) Suzuki–Miyaura coupling.

Our initial studies leveraged our experience using readily available and inexpensive Ni(II) salts as precatalysts for nickel-catalyzed borylation <sup>35,45,51</sup> to develop a screening platform for nickel-catalyzed SMC. As additional design criteria, we sought to identify homogeneous reaction conditions that were broadly suitable for a range of heterocyclic coupling partners. As in our nickel-catalyzed borylation work, the key to realizing these objectives proved to be the use of methanol as a co-solvent. Specifically, we found that a variety of simple mono- and bis-phosphine ligands gave productive cross-coupling for a range of coupling partners with NiCl<sub>2\*</sub>6H<sub>2</sub>O as precatalyst and DBU as an inexpensive, soluble organic base in a mixture of 9:1 2-MeTHF:MeOH or 9:1 DMAc:MeOH at 80 °C (Figure 5).<sup>63</sup> This platform enabled us to successfully identify ligands capable of promoting cross-coupling with a variety of (hetero)aryl chloride, bromide, iodide and triflate electrophiles, and aryl pinacolboronate, aryl neopentylglycolboronate, and (hetero)arylboronic acid nucleophiles. The scalability of the reaction conditions employed in the screening platform was demonstrated by the coupling of the chloride-containing antipsychotic perphenazine on a 6 g scale, which proceeded in 83% yield using 4.5 mol % NiCl<sub>2\*</sub>6H<sub>2</sub>O/DPPF as catalyst (eq 3). Notably, it was observed that the residual Ni was readily purged via simple aqueous washes, resulting in <100 ppm Ni in the isolated product.<sup>64,65</sup>

## Ligands (12):

PPh <sub>3</sub>	DPPE	DCEPhos
DPPF	S-Phos	Ph-XPhos
DCPP	CgMe-PPh	P(p-Anis) <sub>3</sub>
DPPB	A-caPhos	P(3,5-CF <sub>3</sub> -C <sub>6</sub> H <sub>3</sub> ) <sub>3</sub>

Figure 5. Screening platform for Ni-catalyzed C(sp<sup>2</sup>)–C(sp<sup>2</sup>) Suzuki–Miyaura coupling.

Despite the success of the screening platform in generating lead conditions for nickel-catalyzed SMC, we identified several limitations that we sought to improve upon. Because of the high affinity of MeOH for NiX<sub>2</sub> species, there is the potential for displacement of the phosphine ligands from the Ni(II) precatalyst prior to generation of the active catalyst, which could lead to a mixture of different Ni-containing species and catalyst activation pathways. Additionally, there is also the possibility for any ligand-free NiX<sub>2</sub> species to form inactive [Ni(OMe)<sub>2</sub>]<sub>n</sub> oligomers in the presence of base and methanol, as uncovered in our investigations into the diboron-mediated reduction of Ni(II) salts (vide supra).<sup>45</sup> Finally, while the use of DBU and MeOH enabled us to avoid the challenges of insoluble inorganic bases with low water tolerance, it also resulted in the formation of aryl methyl ether species as a byproduct in many cases. Because all of these limitations could be linked to the use of NiCl<sub>2</sub>•6H<sub>2</sub>O as a precatalyst and the requirement of MeOH as a cosolvent for optimal performance, we sought to identify a more robust yet general and widely available nickel precatalyst that would not require an alcohol co-solvent.

While Pd-catalyzed SMCs commonly employ water as a co-solvent, <sup>66</sup> such conditions are rare for nickel. <sup>67</sup> A potential explanation for this is suggested by the elegant mechanistic studies performed by Grimaud and co-workers, which point to the facile formation of off-cycle Ni μ-hydroxo-dimer species that do not readily undergo transmetallation with organoboron nucleophiles. <sup>68</sup> We hypothesized that a weak amine base might enable more robust water-tolerant conditions by minimizing the amount of Ni hydroxide species present in the reaction mixture. To test this hypothesis, we prepared the Ni(DPPB)(*o*-Tol)Cl complex and investigated the effect of base and water on the relative amounts of the L-Ni(Ar)Cl oxidative addition complex and Ni μ-hydroxo dimer species formed in solution. Our studies revealed that these species are in

equilibrium in the presence of DIPEA and solvent quantities of water, thus setting the stage for the development of a catalytic reaction system using these conditions.<sup>69</sup> We were inspired by the development over the past decade of discrete Ni(II) oxidative addition complexes, containing bisphosphine ligands such as DPPF<sup>61b</sup> and DPEphos,<sup>70</sup> which readily enter the catalytic cycle under the SMC reaction conditions. This led us to select Ni(PPh<sub>3</sub>)<sub>2</sub>(o-Tol)Cl as a modular, air-stable and commercially-available precatalyst that enables in situ catalyst generation with a variety of bisphosphines through ligand exchange. In the course of our optimization studies, we determined that the inclusion of neopentyl glycol as a stoichiometric additive often led to a significant increase in the reaction rate, presumably due to in situ formation of a neopentyl glycol boronate ester that undergoes faster transmetallation under the reaction conditions.<sup>71</sup> The conditions shown in Scheme 5 were successfully applied to the coupling of a range of (hetero)aryl chloride and (hetero)arylboronic acid substrates with a variety of functional groups and electronic properties. The methodology was also effective for a number of complex pharmacologically-relevant molecules, including rivaroxaban and perphenazine, with the coupling of the latter compound providing 88% yield on a 50 g scale with just 0.5 mol % Ni.

**Scheme 5**. Ni-catalyzed C(sp²)–C(sp²) Suzuki–Miyaura Coupling with Amine Base and Water as a Cosolvent

*Ni-catalyzed C–N coupling*. In line with the prevalence of C–N couplings throughout the history of our catalysis group, most frequently utilizing palladium catalysts, a current area of focus for our EAM catalysis efforts is in building our capabilities and understanding of nickel-catalyzed C–N coupling processes.

Because these efforts are in a much earlier stage relative to our work in nickel-catalyzed borylation and C(sp<sup>2</sup>)–C(sp<sup>2</sup>) SMC, we will summarize here only briefly some of the challenges and goals for these studies (Figure 6). We also note that, notwithstanding the impressive advances from Prof. Dawei Ma's group and others in the last several decades, 72 the substrate scope for copper-catalyzed C-N coupling is traditionally limited to aryl iodides and bromides, whereas nickel catalysis has shown more promise for engaging less reactive aryl chlorides and phenol derivatives. However, a common limitation for both metals is the frequent use of poorly soluble inorganic bases such as K<sub>2</sub>CO<sub>3</sub>, Cs<sub>2</sub>CO<sub>3</sub> and K<sub>3</sub>PO<sub>4</sub>, which present challenges for scalability and robustness, 73 or strong inorganic bases such as NaOt-Bu and KOt-Bu, which lead to limited functional group tolerance. The field has made significant advances over the last decade based on the development of new methodologies and ligands by the Hartwig, Buchwald, and Stradiotto groups, which demonstrate good functional group tolerability and utilize bench-stable nickel precursors.<sup>74</sup> Notably, the Stradiotto group has elegantly shown that a soluble-dual base strategy<sup>75</sup> can be readily applied to a variety of challenging nickel-catalyzed C-N couplings such as those involving primary and secondary amides<sup>76</sup> and β-fluoroalkylamines.<sup>77</sup> We are now beginning to look at these reaction conditions through the lens of scalability and exploring the importance of the nature of nickel precatalyst, as many are not commercially available. Our strategy remains the same for this bond disconnection: 1) develop the screening platform 2) understand the scalability and 3) continually evaluate for utilization in our portfolio.

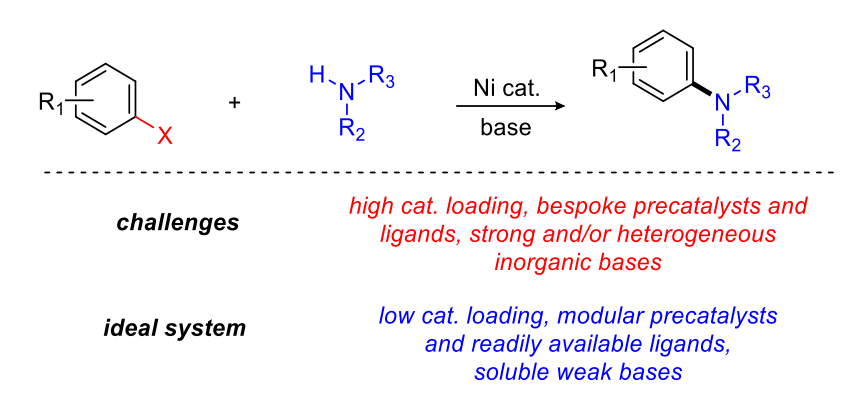


Figure 6. Challenges and design goals for Ni-catalyzed C–N coupling.

As noted above, remarkable advances have recently been made in copper-catalyzed C–N and C–O couplings, due in large part to the work of the Ma group, among others. As a results of these efforts, couplings of aryl iodides and bromides can now be coupled with much lower catalyst loadings and under far milder conditions compared to the original Ullmann–Goldberg reports dating back to the early 1900s, and (hetero)aryl chlorides are now emerging as viable substrates for copper-catalyzed C–X couplings. At BMS, a copper-catalyzed C–N coupling of a heteroaryl bromide was utilized for the development of a commercial synthesis of the HIV attachment inhibitor BMS-663068 (fostemsavir), now marketed as Rukobia by ViiV Healthcare for the treatment of HIV/AIDS. Given our prior experience with large-scale applications of copper catalysis as well as the ongoing advances in the field, we plan to evaluate both copper and nickel catalysts in parallel as alternatives to palladium catalysts for future C–X couplings in the

BMS portfolio, with an eye towards process-friendly conditions employing soluble bases and readily available ligands and precatalysts for each metal.

*Ni(0)* precatalyst development. Through our studies on the nickel-catalyzed C(sp²)–C(sp²) SMC, we learned the importance of evaluating various nickel precatalysts to determine which is ideal for a given transformation. For a nickel-catalyzed borylation, the reduction of a Ni(II) halide precatalyst to an active ligated Ni(0) species is almost instantaneous, and therefore utilizing these simple, easily available Ni(II) halide salts is preferred for these reactions. However, we learned that the formation of [Ni(OMe)₂]n can pose challenges to developing scalable processes with the Ni(II) halide salts, particularly for transformations where the Ni(II) to Ni(0) reduction process is less facile compared to the diboron-mediated pathway. These insights prompted us to reflect on the guiding principles for developing an ideal nickel precatalyst, with initial focus on Ni(0) species, and became a main objective in our on-going collaboration with the Engle lab at The Scripps Research Institute.<sup>79</sup>

The importance of collaborations between academia and industry cannot be overstated. Over the last ten plus years, BMS has collaborated with The Scripps Research Institute across medicinal and process chemistry, where we have driven excellence in industry-academic collaborations to create value, both in terms of scientific knowledge, portfolio value, and future innovations. The collaboration has investigated many facets of chemistry and chemical biology; a significant part of this long-standing collaboration has focused on catalysis with Profs. Yu, Blackmond, and Engle, spanning palladium and EAM such as copper and nickel. Our collaboration with the Yu lab has focused on innovation aimed towards new reaction methodology, mainly mediated by palladium, with a lens toward our discovery team.<sup>80</sup> Multiple transitionmetal catalyzed mechanistic interrogations have been completed with the Blackmond lab, for example impacting the process route to fostemsavir through investigation of an Ullmann coupling<sup>7c</sup> and building understanding of stereospecificity in a rhodium-81 or ruthenium-catalyzed82 hydrogenation relevant to our portfolio. Further, we reported the importance of catalyst activation of palladium(II) precatalysts in the formation of a bis-phosphine mono-oxide palladium complex for a direct arylation from our JAK2 program.<sup>83</sup> This catalyst activation pathway has been realized in several portfolio projects for other palladium-catalyzed transformations, leading to the execution of robust, scalable processes. More recently, a Nature Chemistry comment by Schultz and Campeau from Merck discusses how to bridge the gap between academic and industrial research and how collaborations can impact the field of drug development.84

BMS's goal for academic collaborations with respect to our EAM platform has been to build foundational knowledge across different first-row metals by establishing relationships with leaders in the field to advance mechanistic understanding and develop novel catalysts and transformations that can be applied to the BMS portfolio. Productive collaborations benefit both groups in industry and academia. Our process group has expertise in developing robust, scalable chemistry, and we also have advanced technologies and capabilities such as high-throughput experimentation, automation, and high-speed analytical chemistry to rapidly assess a given transformation. The academic groups have expertise in a specific area of chemistry,

and the ability to investigate novel reactivity with curious, motivated students and post-docs working toward an aligned goal. Academic groups also have access to instrumentation not common in process chemistry (for example, Mössbauer spectroscopy, cryo-EM, low-temperature EPR spectroscopy, magnetic circular dichroism spectroscopy). Furthermore, each group of academic and industrial chemists has their own existing network of collaborators that can be utilized to expand capabilities. For example, we collaborated with solid-state NMR experts to understand the decomposition of metal alkoxides as a project with the Engle lab.<sup>85</sup> In our on-going collaboration on Ni(0) precatalysts, we have collaborated with Song Lin's group to understand the oxidation/reduction potential of these complexes and are currently collaborating on an electrochemical project with Julien Vantourout.

The collaboration between BMS and the Engle lab has been highly productive and encompasses more than nickel catalysis; however, the rest of the collaboration is outside the scope of this perspective. The goal of the Ni-precatalyst project was to find an air-stable replacement for Ni(cod)<sub>2</sub>. Although commonly employed in many transformations, Ni(cod)<sub>2</sub> is not suitable for large-scale manufacturing because of its extreme air sensitivity.<sup>86</sup> Notably, a recent search of OPRD did not yield any examples of Ni(cod)<sub>2</sub> being implemented as a catalyst on kilogram scale. However, the utility and usefulness of Ni(cod)<sub>2</sub> and its impact to the field of nickel catalysis is undeniable. For example, around the same time as the development of the nickel-catalyzed borylation on our BTK inhibitor project, the first BMS process methodology using nickel catalysis was developed.<sup>87</sup> Drawing inspiration from the known reactivity of isatoic anhydrides in cycloadditions,<sup>88</sup> as well as precedent to form atropisomers in similar reactions employing isocyanates with rhodium catalysts,<sup>89</sup> we attempted to synthesize the C–N chiral axis via nickel catalysis (Scheme 6). Although proof-of-concept data was obtained for the synthesis of the necessary fragment in high yield, the correct enantiomer proved challenging to access with high levels of stereoselectivity. However, if a ligand was discovered to overcome the enantioselectivity issue, a replacement for Ni(cod)<sub>2</sub> would be required to scale this chemistry.

Scheme 6. Ni-catalyzed Synthesis of Quinazolinediones from Isatoic Anhydrides and Isocyanates

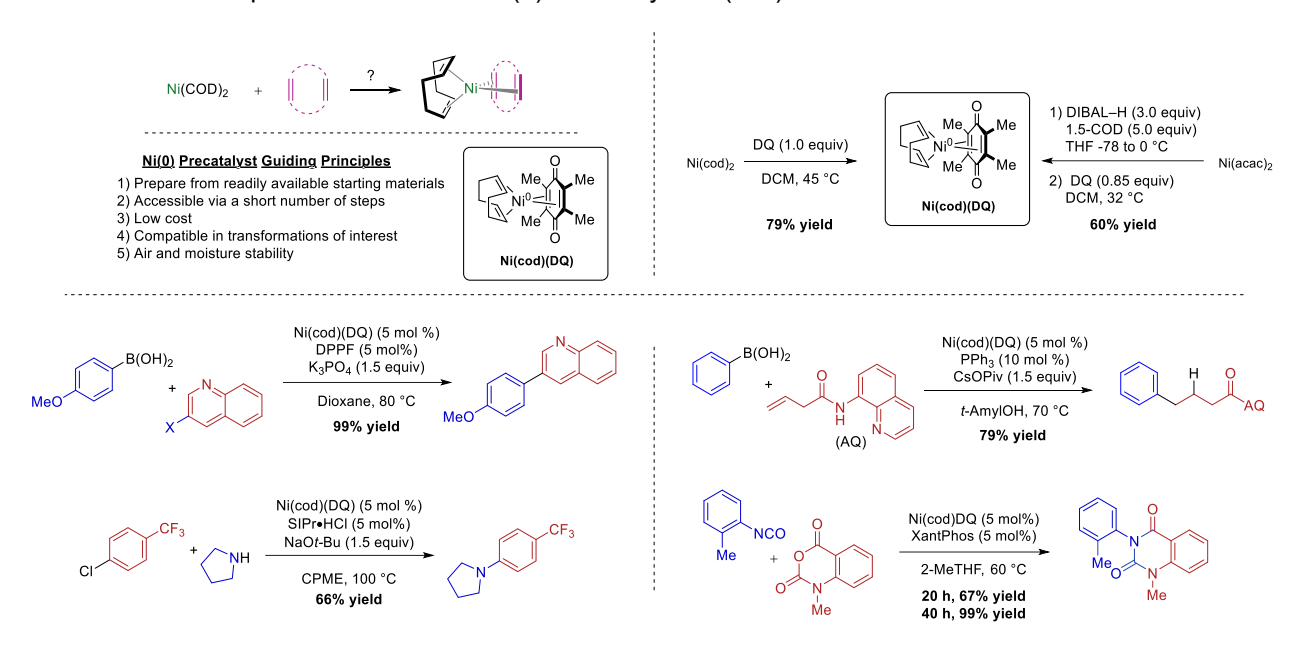
In addition to this example from the BMS portfolio, we realized the broader impact of an air-stable Ni(0) precatalyst across academia and industry. Recently, the Garg lab has demonstrated a wax capsule approach to utilizing Ni(cod)<sub>2</sub>, where the complex is encapsulated in paraffin and handled outside the

glovebox,<sup>90</sup> a strategy first developed by Buchwald for glovebox-free handling of palladium catalysts and cross-coupling reagents.<sup>91</sup> Although this approach is effective for lab scale procedures on the benchtop, it is not feasible for large-scale production of pharmaceutical intermediates. Therefore, we defined guiding principles for a Ni(0) precatalyst: 1) prepared from readily available starting materials, 2) accessibility via a short number of steps, 3) low cost, 4) compatibility in transformations of interest, 5) air and moisture stability. In parallel to our work investigating 18-electron Ni(0) complexes, which builds upon and draws inspiration from the nickel–olefin complex research by Wilke,<sup>92</sup> the Cornella group has reported a series of 16-electron Ni(0) tris(stilbene) precatalysts.<sup>93,94</sup>

Given the widespread use of Ni(cod)<sub>2</sub> in academia, our investigation initially focused on complexes that were isostructural and isoelectronic to Ni(cod)<sub>2</sub>, possessing the same "ligandless" characteristic that allows association of a diverse array of phosphine, NHC, and nitrogen-based ligands. This logic led us to focus attention on Ni(cod)(L) complexes, where the capping ligand L is more strongly coordinating than cod and more electron-withdrawing, thus making the nickel center less prone to oxidation by O<sub>2</sub>, a principal deactivation pathway with Ni(cod)<sub>2</sub> in air. To this end, we explored a series of substitution reactions of Ni(cod)<sub>2</sub> with different monodentate and bidentate capping ligands<sup>95</sup> that were hypothesized to be later displaceable by phosphines or related ligands. We found capping ligands containing an embedded electron-poor diene motif cleanly displaced one equiv of COD, leading to identification of our first lead, Ni(cod)(DQ) (Scheme 7, DQ = duroquinone), a complex first prepared by Schrauzer in the 1960s from Ni(CO)<sub>4</sub><sup>96</sup> but never previously investigated as a precatalyst. Analysis of this complex has shown that it is remarkably thermally stable and robust to air, heat, and water, unlike its precursor, Ni(cod)<sub>2</sub>, thus meeting one of the guiding principles for Ni(0) precatalyst development.<sup>97</sup>

We then sought to determine if Ni(cod)(DQ) would meet the remaining guiding principles. Ni(cod)(DQ) can be prepared from Ni(cod)<sub>2</sub> via the addition of one equiv of DQ; however, for a more scalable approach, it can be readily prepared from Ni(acac)<sub>2</sub>, making it accessible in a short number of steps. In terms of cost, Ni(acac)<sub>2</sub> costs <\$20/mol, demonstrating the low cost to prepare this complex. Further, Ni(cod)(DQ) has been commercialized by MilliporeSigma, Strem, and SinoCompound, and it has been integrated into SinoCompound's "Nickel Acceleration kit." Lastly, Ni(cod)(DQ) was shown to be an effective catalyst in a variety of model transformations spanning different ligands, solvents, bases, temperatures, including SMC, C–N coupling, borylation, C–H activation, and alkene hydroarylation. We were excited to see that Ni(cod)(DQ) could be utilized as replacement for Ni(cod)<sub>2</sub> in a model system for the cyclization from the BTK project (Scheme 7), where a longer reaction time of 40 h led to complete conversion.

Scheme 7. Development of Air-Stable Ni(0) Precatalyst: Ni(cod)DQ



The widespread availability of Ni(cod)(DQ) has facilitated its rapid adoption. As a notable example, Strotman and colleagues at Merck have developed an aryl nitrile isotope exchange reaction that employs Ni(cod)(DQ) as the catalyst of choice. Despite the generality of Ni(cod)(DQ), it is not without limitations. In our most recent work, we have attempted to address limitations of Ni(cod)(DQ), namely the poor reactivity in cases involving more weakly coordinating ligands that are unable to displace DQ and enter the catalytic cycle, by developing a screening kit of structurally diverse Ni(cod)(L) complexes bearing different capping ligands with different coordination properties (Figure 7). With this library of Ni(0) precatalysts, we are continuing to understand their relative physical properties and ability to serve as precursors for an array of chemical transformations.

Figure 7. Ni(0) precatalyst toolkit.

A focus of the collaboration between the Engle lab and BMS has been on the advancement of difunctionalization of alkenes utilizing Ni-catalysis. This endeavor has been very productive, leading to a series of publications and pushing the state of the art in the directing-auxiliary-free diarylation of alkenyl

amides,<sup>101</sup> carboxylates<sup>102</sup> and ketones,<sup>103</sup> for example. Through our work in this field, we learned the importance of an electron-deficient olefin, showcasing the ability of Ni(cod)(DMFU) to serve as a catalyst in challenging diarylations.<sup>104</sup> While the initial goal of the precatalyst project was to develop Ni(0) complexes that were more stable but otherwise functionally equivalent to Ni(cod)<sub>2</sub>, we and others<sup>98c</sup> have found that quinone-ligated nickel centers possess unique reactivity in important reactions, such as the aforementioned difunctionalization of alkenes, or nickel-catalyzed C–N couplings, which is a phenomenon we are now exploring in depth through our collaboration.

Throughout our development of nickel-catalyzed borylations, SMC and C–N couplings, we have focused on scalable, robust reaction conditions. A key component to these methodologies is the choice of nickel precatalyst (Table 3). Although Ni(II) halides are the cheapest, most widely available sources for nickel catalysis, we have learned that they are not ideal for every type of reaction. When catalyst activation is rapid and irreversible, as is the case of borylation reactions, these precursors are very effective. However, in the case of SMC reactions we have found that oxidative addition complexes of nickel allow for low catalyst loading with co-solvent amounts of water. In terms of Ni(0) sources that are commercial, for glovebox usage and small-scale methodology, Ni(cod)<sub>2</sub> has its strengths. However, the development of more air-stable 16-and 18-electron Ni(0) catalysts that have been demonstrated to facilitate a large number of transformations will hopefully transition the field toward the use of these scalable Ni(0) precatalysts. There is additional understanding needed for the Ni(cod)(L) species regarding catalyst activation and applicability toward pharmaceutically relevant substrates, and those studies are currently underway.<sup>105</sup>

Table 3. Comparison for Ni precatalysts.

	Ni(II) salts	Ni(0)(cod)(L) Source	Homoleptic Ni(0) Source	Ni(II) OAC
Benefits	Inexpensive, widely	Obviates challenges of	Obviates challenges of	Air-stable, Ni(II) to Ni(0)
	available, air- and moisture-	Ni(II) to Ni(0) reduction	Ni(II) to Ni(0) reduction	reduction occurs under
	stable			reaction conditions
Limitations	Can be poorly soluble in	Can be air-sensitive,	Can be air-sensitive,	Activation consumes one
	organic solvents, prone to	stabilizing ligands may	stabilizing ligands may	coupling partner and
	formation of $[Ni(OR)_2]_n$	inhibit catalysis	inhibit catalysis	generates organic by-
	oligomers, reduction to Ni(0)			product; ligand exchange
	can be challenging			may not be facile
Availability	Yes	No	No	No*
on kg scale				

Moving left from Group 10. The vast majority of EAM catalysts that have been developed for C(sp²)–C(sp²) SMC to date utilize nickel. While copper catalysts have also been reported,<sup>106</sup> they tend to operate at high temperatures (usually ≥80 °C and often ≥120 °C) and are generally limited to more reactive (and less widely available) aryl iodides or activated aryl bromides.<sup>107</sup> Given these limitations, we considered that earlier first-

row transition metals, such as cobalt and iron, might possess untapped potential for SMC with possibly milder conditions and broader scope. However, there are several additional challenges to contend with when working with first-row metals that lie to the left of nickel on the periodic table. Because of their increased oxophilicity, cobalt and iron have a higher propensity toward catalyst deactivation by aggregation of metal hydroxide and alkoxide complexes. Cobalt and iron complexes are also more likely to exist in high-spin states compared to nickel, which adds another layer of complexity and can limit the application of traditional spectroscopic tools such as NMR. Below we briefly highlight a pair of studies from the Chirik group related to cobalt and iron-catalyzed SMC, which illustrate some of the challenges and unique features of earlier first-row metals and also provided key learnings that influenced the research focus for our subsequent collaboration.

Transmetallation to Co(I) and Co-catalyzed C(sp<sup>2</sup>)-C(sp<sup>2</sup>) Suzuki-Miyaura coupling. In a prelude to the formal collaboration between BMS and the Chirik group, studies conducted in the Chirik lab with funding by the ACS Green Chemistry Institute Pharmaceutical Roundtable showed that a well-defined cobalt bis(phosphino)pyridine (PNP) pincer complex could undergo stoichiometric transmetallation from boron to cobalt with neutral organoboron reagents. Furthermore, this complex was also capable of promoting catalytic C(sp<sup>2</sup>)–C(sp<sup>2</sup>) SMC of a series of aryl triflates and heteroarylboronate esters under relatively mild conditions (Scheme 8a). 109 Although the substrate scope was modest, this was the first cobalt catalyst that had been shown to promote catalytic C(sp2)-C(sp2) SMC. Notably, the starting (PNP)Co(I) alkoxide complex is a tetrahedral, high-spin species whereas the product of transmetallation is a planar, diamagnetic low-spin Co(I) complex, suggesting spin state changes may occur during the catalytic cycle. Subsequent to this initial report, work by the Duong group using a Co(II)/terpyridine catalyst system expanded the scope of Co-catalyzed C(sp<sup>2</sup>)-C(sp<sup>2</sup>) SMC to include a variety of (hetero)arylboronic esters and (hetero)aryl halides (Scheme 8b). 110 Key to the success of the reactions reported by Duong was the use of KOMe as base and aryl neopentyl glycolboronate nucleophiles. Subsequent to the initiation of the BMS-Chirik collaboration in 2019, the Bedford group in 2021 disclosed a Co(II)/NHC catalyst for the coupling of aryl chlorides and aryl neopentyl glycolboronates (Scheme 8c). 108e The Chirik and Duong studies provided important insights into Co catalysis that were influential in our initial work to develop catalysts for Cocatalyzed C(sp<sup>2</sup>)–C(sp<sup>3</sup>) SMC (vide infra), while the Bedford studies revealed a number of key trends, such as the importance of the relative stoichiometries of base and arylboron species, which we have also observed and applied in our own work.

# Scheme 8. Co-catalyzed C(sp<sup>2</sup>)–C(sp<sup>2</sup>) Suzuki–Miyaura Coupling

Transmetallation of neutral arylboronate esters to Fe(II) complexes. The Chirik group also demonstrated the first transmetallation of neutral organoboronate ester nucleophiles to an iron alkoxide complex (Scheme 9). The ( $^{\text{iPr}}$ PDI)FeOEt complex, prepared by protonolysis of an iron alkyl precursor with ethanol, undergoes rapid transmetallation with both (2-benzofuranyl)BPin and (2-benzofuranyl)BNeo in C<sub>6</sub>D<sub>6</sub> at room temperature. As previously observed with cobalt, this transmetallation is accompanied by a change in the spin state of the iron complex from high-spin (S = 3/2) to low-spin (S = 1/2). It is also noteworthy that the iron alkoxide complex was monomeric and did not undergo aggregation. While the resulting ( $^{\text{iPr}}$ PDI)FeOEt(aryl) complex was found to undergo facile conversion to ( $^{\text{iPr}}$ PDI)FeX<sub>2</sub> complexes upon reaction with a variety of aryl and alkyl halide electrophiles, accompanied by low yields (<15%) of crosscoupled product, this work was critical in laying a foundation for the application of Suzuki-type transmetallation from boron to iron with neutral organoboronate nucleophiles in the future development of iron-catalyzed C(sp²)–C(sp³) cross coupling methods (vide infra).

Scheme 9. Transmetallation of Neutral Organoboronate Esters to an Iron(II) Alkoxide Complex

Me Ar

N-Fe-OEt + 
$$(RO)_2B$$

N-Fe

### New transformations enabled by Earth-abundant metals

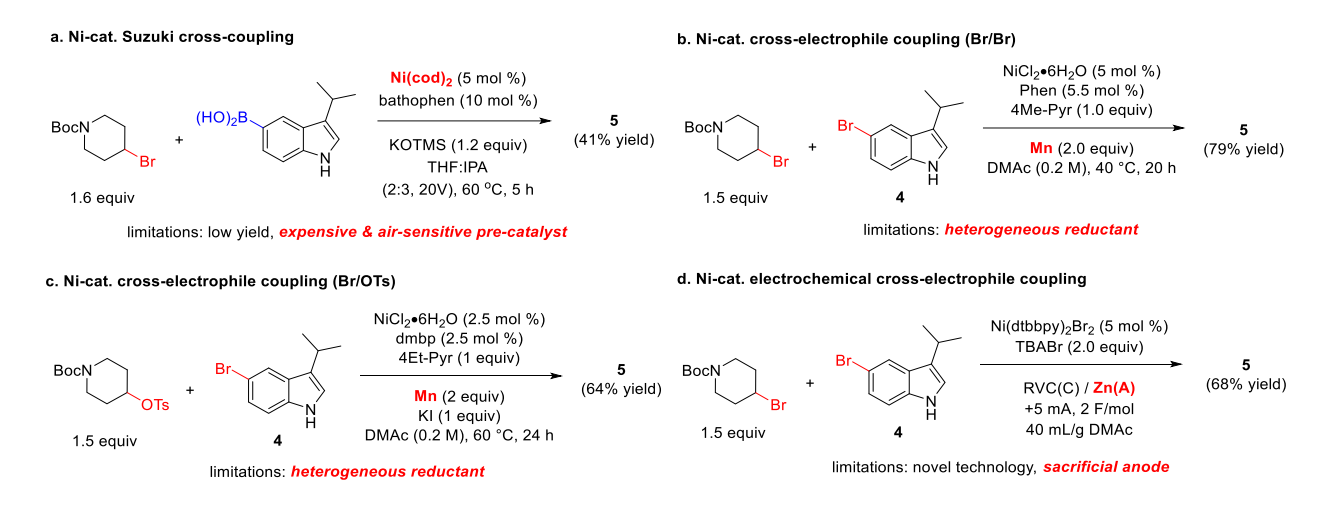
As noted in the introduction, a complementary driver for building capabilities with EAMs lies in their ability to mediate transformations that are challenging or not currently possible with precious metals, such as palladium. While the nickel-catalyzed borylation of less reactive aryl sulfamate electrophiles (vide supra) can be considered to fall under this umbrella from the perspective of being a challenging C(sp²)–O bond *cleavage* for palladium, we note that the type of bond that is *formed* in this process (i.e., C(sp²)–B) is extremely well established for palladium catalysis. In contrast, both the cleavage of C(sp³)–X bonds and the formation of C(sp²)–C(sp³) bonds are generally challenging with palladium, <sup>112</sup> often requiring highly reactive nucleophiles such as organomagnesium or organoborane species, <sup>113</sup> and with the substrate scope almost exclusively limited to primary C(sp³)–X electrophiles. <sup>10</sup> On the other hand, a number of examples employing more synthetically valuable secondary C(sp³)–X electrophiles have been reported using EAM such as nickel, <sup>114</sup> including BMS's collaboration with the Baran lab on the develop of the C(sp²)–C(sp³) cross-coupling of redox-active esters. <sup>115</sup> Combined with recent reports of the preparation of more complex C(sp³)–X electrophiles utilizing EAM, <sup>116</sup> such as the BMS collaboration with the Yu lab on the coppercatalyzed bromination of C(sp³)–H bonds, <sup>117</sup> the ability to assemble and elaborate complex, pharmaceutically-relevant substrates has greatly expanded in the last few years.

Our interest in identifying mild methods for C(sp²)–C(sp³) bond formation was driven by both the ongoing general shift toward C(sp³)-rich molecules in the medicinal chemistry community, which has been correlated with increased chances of success in the clinic¹¹¹³ and improved solubility,¹¹¹¹ as well as by the specific needs of our own internal portfolio. In particular, the identification of a series of antagonists of toll-like receptors 7/8/9 (TLR 7/8/9) by our BMS discovery colleagues¹²⁰ prompted us to undertake a systematic evaluation and critical comparison of known methods for C(sp²)–C(sp³) bond construction in the context of the synthesis of indole 5 (Scheme 10).¹²¹ This core structure was originally prepared by a two-step sequence involving palladium-catalyzed C(sp²)–C(sp²) SMC of bromoindole 4 and a commercially available alkenyl-B(pin) coupling partner, followed by palladium-catalyzed reduction of the newly introduced alkene.¹²⁰ We were encouraged to find that several existing technologies enabled installation of the C(sp²)–C(sp³) bond in a single step, namely nickel-catalyzed SMC, nickel-catalyzed cross-electrophile coupling, and nickel-catalyzed electrochemical coupling. We subsequently investigated each transformation in detail to determine how effective they would be for the forging the key C(sp²)–C(sp³) bond under optimized conditions and how amenable each process would be to implementation on a large scale.

Scheme 10. Original Two-step Synthesis of TLR 7/8/9 Antagonist Indole Core 5

Optimization of the nickel-catalyzed SMC was based around the work of the Fu group, where the use of alkoxide bases together with N,N-ligands forged C(sp<sup>2</sup>)–C(sp<sup>3</sup>) bonds in high yield. 122 For the challenging coupling from our portfolio, we were able to develop reaction conditions that provided the desired product in a modest 41% yield (Scheme 11a). In addition to the low yield, this transformation utilized Ni(cod)2 as the precatalyst, which is unsuitable for scale-up for reasons explained earlier in this perspective. Two separate cross-electrophile couplings were then investigated, both utilizing bromoindole 4 as one electrophilic partner and either the piperidinyl bromide<sup>123</sup> or piperidinyl tosylate<sup>124</sup> as the other partner. The alkyl bromide performed moderately better than the alkyl tosylate (79% vs 64%, Scheme 11b-c); however, both reaction conditions utilize Mn<sup>0</sup> as a stoichiometric reductant, as we were unable to find a soluble reductant that worked well for this transformation. Although we previously scaled a cross-electrophile coupling to 7 kg with our colleagues at BBRC, this reaction was performed in specialized equipment to ensure proper mixing of the dense, solid Mn<sup>0</sup>, and this was the highest scale the reaction could be performed. 125 Therefore, there are scale limitations of this transformation when using stoichiometric heterogeneous reductants, 126 in addition to the moderate-to-good yields obtained with our specific coupling. The electrochemical cross-electrophile coupling was also investigated in detail with a series of substrates. 127 One key learning was that the reaction performs best with the same halide on both coupling partners as well as the electrolyte to prevent scrambling of the halides on the electrophiles. Although 68% yield was obtained for this method (Scheme 11d), the implementation of these conditions on large scale would require the use of novel technology as well as a sacrificial anode (and subsequent stoichiometric salt).

**Scheme 11**. Application of Known Methods for C(sp<sup>2</sup>)–C(sp<sup>3</sup>) Bond Construction to the Synthesis of Indole **5** 



After extensive efforts to apply these known methodologies to our challenging transformation, we concluded that the operational concerns of the new technologies did not outweigh the benefits of having a direct, single-step bond formation in this case. It is important to note that these transformations are vitally important for the advancement of the field and that our specific transformation proved to be among the most

challenging examples. We will continue to investigate these transformations whenever we can apply them to our portfolio. In a similar vein, through the same disconnection one could envision a series of metallaphotoredox transformations to forge the desired for C(sp²)–C(sp³) bond.²² Unfortunately, screening with the alkyl- and heteroaryl bromide coupling partners in a metallaphotoredox reductive coupling manifold with the reported Ni/Ir dual catalytic system¹²² was not very successful and afforded the product in only 47 LCAP.¹²¹ Alternatively, a decarboxylative coupling¹²² with the heteroaryl bromide and alkyl acid coupling partner was investigated with a series of photocatalysts, and even with *N*-Boc protection of the indole (which was required for any appreciable reactivity), the highest amount of product observed was 34 LCAP.¹²¹

Our team has continued to investigate this key bond formation utilizing metallaphotoredox transformations, with a focus on identifying new bond-forming technologies as well as improvements to the conditions for existing technologies. Through a collaboration with our colleagues in discovery chemistry, we developed a Ni/photoredox-catalyzed coupling of alkyl pinacolboronates and (hetero)arylbromides that can operate in both batch and flow modes. When applied to the synthesis of the TLR indole core, these conditions afford the desired cross-coupled product 5 in 78% solution yield (eq 4) with low catalyst loadings of an inexpensive Ni(II) salt and pyridyl-imidazole ligand and an organic photoredox catalyst, providing a promising path forward for utilizing metallaphotoredox catalysis on difficult C(sp²)–C(sp³) bond formations.

Co-catalyzed  $C(sp^2)$ – $C(sp^3)$  Suzuki–Miyaura coupling. After a thorough examination of the state-of-the-art methods for forging  $C(sp^2)$ – $C(sp^3)$  bonds utilizing nickel catalysis with potentially scalable reaction conditions, it was clear that there was a need for further exploration into this type of bond formation. To that end, we started a collaboration with Paul Chirik at Princeton University, with the goal of developing novel methodology utilizing EAMs. We decided to investigate whether cobalt would be a viable catalyst for  $C(sp^2)$ – $C(sp^3)$  SMC, which had not yet been demonstrated in the literature. The collaboration began with the design of a substrate ladder of nucleophile and electrophile pairs, where each step of the ladder increases complexity with the top step being our desired  $C(sp^2)$ – $C(sp^3)$  coupling reaction (Figure 8). While primary and secondary aliphatic alkyl halides are the most common electrophiles reported in the literature with copper<sup>132</sup> and nickel catalysts for  $C(sp^2)$ – $C(sp^3)$  SMC, we were cognizant of the ubiquity of saturated heterocyclic rings, <sup>133</sup> most notably piperidines, <sup>134</sup> in small molecule drugs. Accordingly, we chose to start at the middle of the ladder with the coupling of a piperidinyl bromide electrophile and an electron-neutral phenyl boronate nucleophile, which allowed us to focus on understanding the importance of the class variables in the reaction with pharmaceutically-relevant coupling partners.

Figure 8. Substrate ladder for C(sp<sup>2</sup>)–C(sp<sup>3</sup>) cross-coupling.

Optimization of this transformation led to the discovery of the first-generation system for cobalt-catalyzed C(sp²)–C(sp³) SMC, which utilized *trans-N,N'*-dimethylcyclohexane-1,2-diamine (DMCyDA) as a ligand for this reaction (Scheme 12). The discrete catalytic precursor (DMCyDA)CoBr² could be readily prepared to simplify reaction setup. This complex, along with KOMe as the base in DMAc, afforded the desired coupling across a range of substrates in 37–73% yield. Interestingly, other diamine ligands were unsuccessful in this reaction with yields of <40%. The use of neopentyl glycol boronate nucleophiles was vital for productive catalysis, as both phenylboronic acid and phenylpinacol boronate ester afforded the product in 11% and 5% yield, respectively, under the standard reaction conditions. We were also able to build preliminary understanding of impurity formation, wherein the elimination product is a background reaction from the alkoxide base and bromopiperidine, and the reduction product presumably occurs from quenching of the alkyl radical before it undergoes cross coupling.

Scheme 12. Conditions for the First-Generation (Diamine)Co-Catalyzed C(sp<sup>2</sup>)–C(sp<sup>3</sup>) Cross-Coupling

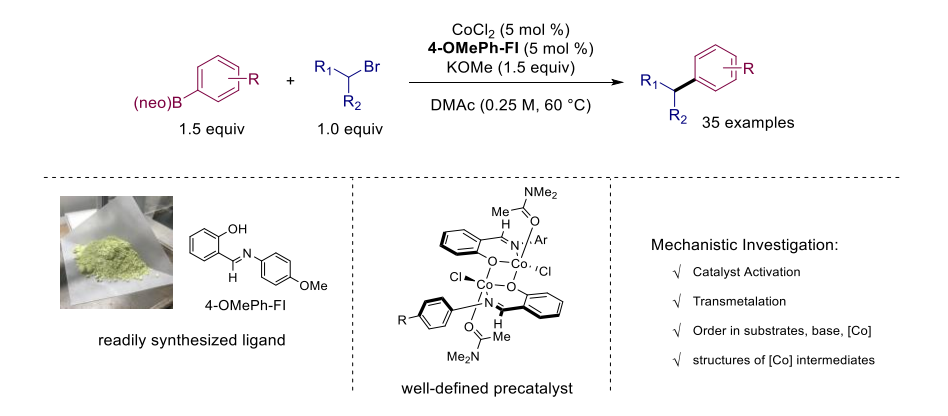
The DMCyDA-CoBr<sub>2</sub> system demonstrated that cobalt could facilitate a C(sp<sup>2</sup>)–C(sp<sup>3</sup>) SMC reaction; however, there were several limitations with this first-generation system. In addition to the high catalyst loading of 15 mol %, the exact nature of the active catalyst was ill-defined. Furthermore, analysis of the reaction profiles indicated a significant amount of C-Br reduction by-product, suggesting that the cobalt effectively generates the alkyl radical but hydrogen atom abstraction from the solvent is competitive with alkyl radical capture and productive cross-coupling. Therefore, we set out to expand our evaluation of the ligand space by exploring additional N,N ligands (bipyridine, diamine), as well as various N,O ligands including 8-hydroxyquinoline (QNOL) derivatives. To conduct these studies rapidly and efficiently, we leveraged the HTE capabilities at BMS, highlighting a powerful capability that industrial partners are often uniquely able to bring to industry-academia collaborations. We were pleased to see that relative to the DMCvDA, the L.X-type N,O ligand 2,5,7-trimethyl-QNOL afforded the product in similar yield with only 4% of the reduction product (relative to 18% with the diamine). The background elimination accounted for the remaining mass balance, suggesting that L,X-type N,O ligands were a promising new ligand class for this transformation meriting further exploration. Evaluation of a broader set of L,X-type N,O-ligands revealed that one class in particular led to generally high conversion to desired product with low reduction by-product at 5 mol % catalyst loading: phenoxyimine (FI) ligands (Scheme 13). 136 It should be noted that these ligands have previously been utilized in early transition metal "post metallocene" polymerization catalysts. 137

**Scheme 13**. Evolution Toward L,X-type N,O Ligands for Co-catalyzed C(sp<sup>2</sup>)–C(sp<sup>3</sup>) Suzuki–Miyaura Coupling

The (FI)Co-catalyzed C(sp²)–C(sp³) SMC shows a broader substrate scope compared to the first-generation diamine system, and the reactions can also be conducted with lower catalyst loadings and well-defined precatalysts (Scheme 14). In preliminary mechanistic investigations, radical clock and trapping experiments are consistent with the intermediacy of electrophile-derived radicals in these couplings, and we have evidence suggesting the formation of borate species under the reaction conditions, although their role is unclear. Nonetheless, a number of mechanistic questions remain, including 1) the mechanism of catalyst activation, 2) the mechanism of transmetallation, 3) the order in each substrate as well as the

base and cobalt catalyst and 4) the structure of [Co] intermediates. Detailed mechanistic studies of (FI)Co-catalyzed  $C(sp^2)$ – $C(sp^3)$  SMC are currently underway, and we look forward to sharing the results of this work in due course.

**Scheme 14**. Second-Generation (FI)Co-catalyzed C(sp<sup>2</sup>)–C(sp<sup>3</sup>) Suzuki–Miyaura Coupling and Key Mechanistic Questions



Fe-catalyzed C(sp²)–C(sp³) Suzuki–Miyaura coupling. In addition to nickel and copper, iron catalysts have also been reported to catalyze C(sp²)–C(sp³) Suzuki-type cross coupling of organoboron species, albeit with some limitations. In 2009, Bedford and coworkers reported the iron-catalyzed cross-coupling of benzyl bromides with sodium and potassium tetraarylborates (only one of the four aryl groups undergoes productive coupling), with the arylborate species employed in a slight excess (1.25 equiv). <sup>138</sup> In 2010, the Nakamura group demonstrated that lithium alkyl borates, prepared from aryl- and alkenylboronic acid pinacol esters and a stoichiometric alkyllithium activator (*t*-BuLi or *n*-BuLi), can undergo iron-catalyzed cross coupling with alkyl halides in the presence of a magnesium(II) halide additive using a bulky bisphosphine ligand. <sup>139</sup> Bedford and coworkers subsequently showed that the couplings of *t*-BuLi-derived lithium alkyl borates could be conducted with simple bis-phosphine ligands or with Fe(acac)<sub>3</sub> with no added ligand. <sup>140</sup> However, the requirement of a stoichiometric amount of a pyrophoric alkyllithium species <sup>141</sup> for activation of the organoboron species presents significant safety concerns for large-scale operation and effectively negates several of the principal advantages of SMC compared to other cross-coupling methods, namely the ease of handling and air- and moisture-tolerance of the nucleophilic species.

The current state of the art in iron-catalyzed C(sp²)–C(sp³) SMC is arguably the catalyst system recently developed by Byers and co-workers, which is the first to allow the direct use of neutral, unactivated arylboronic esters. The Byers catalysts are based on L,X-type N,N ligands and utilize LiNMeEt as base in benzene solvent (Scheme 15a). Unfortunately, the use of a strong, non-commercially available lithium amide base and a highly toxic solvent pose significant barriers for utilization of this technology in large-scale applications. Inspired by our success with (FI)Co-catalyzed C(sp²)–C(sp³) SMC, as well as previous studies in the Chirik group demonstrating stoichiometric boron to iron transmetallation from neutral organoboronate esters (Bneo, Bpin) to discrete iron alkoxide complexes (vide supra), 111 we sought to

determine whether FI ligands might enable iron-catalyzed C(sp<sup>2</sup>)–C(sp<sup>3</sup>) SMC using milder alkoxide bases.<sup>143</sup> After evaluating a series of (FI)Fe(alkyl) complexes as precatalysts, we successfully identified conditions that enable both aryl pinacol boronate and aryl neopentyl glycol boronate esters to be coupled with a variety of alkyl halides (Scheme 15b).<sup>144</sup>

Scheme 15. Fe-catalyzed C(sp<sup>2</sup>)–C(sp<sup>3</sup>) Suzuki–Miyaura Coupling

Outlook. Although the C(sp<sup>2</sup>)–C(sp<sup>3</sup>) cross-coupling has precedent with nickel (as well as palladium, copper and iron), developing complementary methodologies with other available metals is important to drive the EAM field forward. Each methodology has its own strengths and weaknesses in terms of substrate scope capability. There is no universal methodology for C(sp<sup>2</sup>)-C(sp<sup>3</sup>) cross-coupling, and it is not a solved problem, especially in the context of complex pharmaceutically relevant substrates for the cross-coupling. While the cobalt and iron catalysts developed to date though the BMS-Chirik collaboration are not yet capable of effecting C(sp<sup>2</sup>)–C(sp<sup>3</sup>) cross-coupling with unprotected indole substrates, these systems have not yet reached the maturity of the more established nickel systems and thus a head-to-head comparison is still premature. It should also be noted that while organoboronic acids and pinacol boronate esters are more commercially available compared to other organoboron derivatives, many routes to drug candidates require de novo synthesis of a functionally complex boronate species that then undergoes further transformation. The optionality at this stage to investigate the borylation and subsequent reactivity with various organoboron species, including boronic acids, pinacol boronate esters, and neopentyl glycol boronates, is an important process to develop the most synthetically useful route to a given drug candidate. Although the preparation of boronic acids utilizing tetrahydroxydiboron is the most sustainable in terms of atom economy, 145 the per mole cost of each diboron reagent is similar, and the choice of boronate for each project is more impacted by stability and reactivity of the specific organoboronate species. Therefore, continuing to investigate these transformations is a shared responsibility from academia and industry to continue to move the field forward and allow for these impactful, novel transformations to be utilized on kilogram scale routes to drug candidates.

Another important aspect when developing this chemistry is the sustainability of all parts of the reaction—from solvent to base to ligand to metal.3 The focus of our initial efforts at BMS has been on the advantages of utilizing EAMs in place of less abundant metals, such as palladium, mainly because both systems (in the context of the methodologies we have developed with C(sp<sup>2</sup>)-X electrophiles) rely on phosphine ligands to catalyze the desired transformation. However, when we compare sustainability across various methodologies with different EAMs, we can also analyze the impact of ligand choice. Perhaps unsurprisingly, there is a direct correlation between the process mass intensity<sup>146</sup> (PMI, kg of total material used to produce 1 kg of product) and cost.<sup>147</sup> This same analysis can also be applied to the synthesis of ligands. We generally do not think about the routes to ligands but rather whether they are commercially available or not, but in the case of the C(sp<sup>2</sup>)-C(sp<sup>3</sup>) cross-coupling methodologies discussed in this Perspective, there is a dramatic difference in the complexity of the ligand syntheses. For example, in our studies on the application of this methodology to the TLR 7/8/9 core, the top ligand for the nickel-catalyzed cross-coupling was bathophenanthroline. 121 Although commercially available, this ligand costs \$4840/kg and is prepared in three steps in moderate yield (Table 4). The overall PMI for this ligand synthesis, which also uses harsh reaction conditions, is >50.148 Alternatively, the FI ligands can be prepared in a single step using inexpensive, easily sourced starting materials, and the purification is a direct-drop crystallization in methanol. Simply mixing the two reagents, aging, and filtering yields the desired ligand in 90% yield with a PMI of 7.6, demonstrating the increased sustainability from utilizing these ligands. The ease of this synthesis makes FI ligands attractable for large scale synthesis. A library of FI ligands can also be readily prepared using this approach.

**Table 4**. Comparison ligands for Ni- and Co-catalyzed C(sp<sup>2</sup>)–C(sp<sup>3</sup>) SMC.

	Ni catalysis	Co catalysis	
Ligand	Bathophenanthroline <sup>149</sup>	4-OMePh-FI	
Synthetic Route	NO <sub>2</sub> 1) H <sub>3</sub> AsO <sub>4</sub> /H <sub>2</sub> SO <sub>4</sub> (100 °C) Ph NH <sub>2</sub> 2) O NO <sub>2</sub> AcOH, 60° C then N Ph 1) H <sub>3</sub> AsO <sub>4</sub> /H <sub>3</sub> PO <sub>4</sub> (100 °C) Ph NO <sub>2</sub> NO <sub>2</sub> NO <sub>2</sub> AcOH, 60° C then N NO <sub>3</sub> NO <sub>4</sub> NO <sub>4</sub> NO <sub>4</sub> NO <sub>5</sub> NO	↑ OH	
Number of steps	3	1	
Yield (PMI)	15% (>50)	90% (7.6)	
Commercial			
Availability	Yes	No	
Cost	\$4840/kg <sup>a</sup>	\$15/kg <sup>b</sup>	

<sup>&</sup>lt;sup>a</sup> Cost based on the lowest price listed from catalog vendor websites <sup>b</sup> Estimated cost based on the raw materials used to synthesize 4-OMePh-FI

Metric based decisions, utilizing factors like cost, greenness, <sup>150</sup> PMI, number of steps, etc., are at the core of process development. The ability to use EAM catalysis has positive implications in each of those metrics. We set out to build an EAM platform within the BMS process chemistry group by strategically choosing a transformation, building a screening platform and mechanistic understanding, and then investigating applications to our portfolio. Over the span of a few years, we have established the ability to implement several different examples of EAM catalysis on kilogram scale in our portfolio.

The advancement of EAM catalysis in the last decade has been remarkable. As a field, we are just starting to break the ice on fundamental understanding of these underexplored modes of catalysis, and the future is very bright. Discovering new reactivity of EAMs to impact the way in which complex molecules are assembled is only one promising future for EAMs. The ability to expand current methodologies, such as those discussed in this perspective, is another. Miyaura borylation reactions, Suzuki–Miyarua couplings, and C–N couplings will continue to be vital to developing scalable routes to drug candidates, and continuing to improve the robustness, catalyst loading, and substrate scope compatibility is needed for EAM catalysis to become the go-to way to forge these bonds in industry.

Perhaps most importantly, no group can do it alone in academia or industry. The goal of this perspective was to not only explain the philosophy and development of EAM catalysis at BMS but to showcase the importance of collaboration: both internal and external to BMS. Within BMS, we have established strong ties among the network of catalysis experts in the process development group as well as with our discovery colleagues to understand the future portfolio. The real-world chemical challenges of industry can help frame critical and fundamental questions of reactivity—partnership between industrial and academic minds is critical to solving these challenges, and when we work together, the possibilities are endless.

## Acknowledgements

We have been extremely fortunate to work with a number of incredibly talented scientists though our partnerships with academic groups, including the graduate students and postdocs in our collaborations with the Chirik and Engle labs as well as the graduate and undergraduate students from the Frantz lab who helped us explore palladium and nickel-catalyzed borylation reactions. We are grateful for the dedication and contributions of the members of the BMS Catalysis Community of Practice who have helped to the build the platforms and mechanistic understandings discussed in this Perspective. We would like to thank Dr. Francisco González-Bobes, Dr. Martin Eastgate, Dr. Rodney Parsons and the Chemical Process Development Senior Leadership Team for the continued support of our efforts in Earth-abundant metal catalysis and Dr. Matthew Joannou for providing a critical reading of this manuscript. Work on nickel-catalysis in the Engle lab at Scripps Research, including the development of bench-stable Ni(0)

precatalysts, was supported by BMS and the NSF (CHE1800280; CHE-2102550). Work on cobalt and iron catalysis in the Chirik lab at Princeton was supported by BMS through the Princeton Catalysis Initiative.

#### References

- (1) Buskes, M. J.; Blanco, M.-J. Impact of Cross-Coupling Reactions in Drug Discovery and Development. *Molecules* **2020**, *25*, 3493.
- (2) Johansson Seechurn, C. C. C.; Kitching, M. O.; Colacot, T. J.; Snieckus, V. Palladium-Catalyzed Cross-Coupling: A Historical Contextual Perspective to the 2010 Nobel Prize. *Angew. Chem. Int. Ed.* **2012**, *51*, 5062-5085.
- (3) Hayler, J. D.; Leahy, D. K.; Simmons, E. M. A Pharmaceutical Industry Perspective on Sustainable Metal Catalysis. *Organometallics* **2019**, *38*, 36-46.
- (4) (a) Roughley, S. D.; Jordan, A. M. The Medicinal Chemist's Toolbox: An Analysis of Reactions Used in the Pursuit of Drug Candidates. *J. Med. Chem.* **2011**, *54*, 3451-3479; (b) Schneider, N.; Lowe, D. M.; Sayle, R. A.; Tarselli, M. A.; Landrum, G. A. Big Data from Pharmaceutical Patents: A Computational Analysis of Medicinal Chemists' Bread and Butter. *J. Med. Chem.* **2016**, *59*, 4385-4402.
- (5) Dombrowski, A. W.; Aguirre, A. L.; Shrestha, A.; Sarris, K. A.; Wang, Y. The Chosen Few: Parallel Library Reaction Methodologies for Drug Discovery. *J. Org. Chem.* **2022**, *87*, 1880-1897.
- (6) Magano, J.; Dunetz, J. R. Large-Scale Applications of Transition Metal-Catalyzed Couplings for the Synthesis of Pharmaceuticals. *Chem. Rev.* **2011**, *111*, 2177-2250.
- (a) Leahy, D. K.; Fan, Y.; Desai, L. V.; Chan, C.; Zhu, J.; Luo, G.; Chen, L.; Hanson, R. L.; Sugiyama, M.; Rosner, T.; Cuniere, N.; Guo, Z.; Hsiao, Y.; Gao, Q. Efficient and Scalable Enantioselective Synthesis of a CGRP Antagonist. Org. Lett. 2012, 14, 4938-4941; (b) Humphrey, G. R.; Dalby, S. M.; Andreani, T.; Xiang, B.; Luzung, M. R.; Song, Z. J.; Shevlin, M.; Christensen, M.; Belyk, K. M.; Tschaen, D. M. Asymmetric Synthesis of Letermovir Using a Novel Phase-Transfer-Catalyzed Aza-Michael Reaction. Org. Process Res. Dev. 2016, 20, 1097-1103; (c) Gallagher, W. P.; Soumeillant, M.; Chen, K.; Fox, R. J.; Hsiao, Y.; Mack, B.; Iyer, V.; Fan, J.; Zhu, J.; Beutner, G.; Silverman, S. M.; Fanfair, D. D.; Glace, A. W.; Freitag, A.; Sweeney, J.; Ji, Y.; Blackmond, D. G.; Eastgate, M. D.; Conlon, D. A. Preparation of the HIV Attachment Inhibitor BMS-663068. Part 7. Development of a Regioselective Ullmann-Goldberg-Buchwald Reaction. Org. Process Res. Dev. 2017, 21, 1156-1165; (d) Wang, T.; Phillips, E. M.; Dalby, S. M.; Sirota, E.; Axnanda, S.; Shultz, C. S.; Patel, P.; Waldman, J. H.; Alwedi, E.; Wang, X.; Zawatzky, K.; Chow, M.: Padivitage, N.: Weisel, M.: Whittington, M.: Duan, J.: Lu, T. Manufacturing Process Development for Belzutifan, Part 5: A Streamlined Fluorination-Dynamic Kinetic Resolution Process. Org. Process Res. Dev. 2022, 26, 543-550; (e) Treitler, D. S.; Soumeillant, M. C.; Simmons, E. M.; Lin, D.; Inankur, B.; Rogers, A. J.; Dummeldinger, M.; Kolotuchin, S.; Chan, C.; Li, J.; Freitag, A.; Lora Gonzalez, F.; Smith, M. J.; Sfouggatakis, C.; Wang, J.; Benkovics, T.; Deerberg, J.; Simpson, J. H.; Chen, K.; Tymonko, S. Development of a Commercial Process for Deucravacitinib, a Deuterated API for TYK2 Inhibition. Org. Process Res. Dev. 2022, 26, 1202-1222.
- (8) Campeau, L.-C.; Hazari, N. Cross-Coupling and Related Reactions: Connecting Past Success to the Development of New Reactions for the Future. *Organometallics* **2019**, *38*, 3-35.
- (9) (a) Schmink, J. R.; Bellomo, A.; Berritt, S. Scientist-led High-Throughput Experimentation (HTE) and its utility in academia and industry. *Aldrichimica Acta* **2013**, *46*, 71-80; (b) Selekman, J. A.; Qiu, J.; Tran, K.; Stevens, J.; Rosso, V.; Simmons, E.; Xiao, Y.; Janey, J. High-Throughput Automation in Chemical Process Development. *Annu. Rev. Chem. Biomol. Eng.* **2017**, *8*, 525-547; (c) Mennen, S. M.; Alhambra, C.; Allen, C. L.; Barberis, M.; Berritt, S.; Brandt, T. A.; Campbell, A. D.; Castañón, J.; Cherney, A. H.; Christensen, M.; Damon, D. B.; Eugenio de Diego, J.; García-Cerrada, S.; García-Losada, P.; Haro, R.; Janey, J.; Leitch, D. C.; Li, L.; Liu, F.; Lobben, P. C.; MacMillan, D. W. C.; Magano, J.; McInturff, E.; Monfette, S.; Post, R. J.; Schultz, D.; Sitter, B. J.; Stevens, J. M.; Strambeanu, I. I.; Twilton, J.; Wang, K.; Zajac, M. A. The Evolution of High-Throughput Experimentation in Pharmaceutical Development and Perspectives on the Future. *Org. Process Res. Dev.* **2019**, *23*, 1213-1242.
- (10) Pagett, A. B.; Lloyd-Jones, G. C. In *Organic Reactions*; John Wiley & Sons, Inc.: 2020; Vol. 100, p 547-620.
- (11) Hartwig, J. F.; Shaughnessy, K. H.; Shekhar, S.; Green, R. A. In *Organic Reactions* 2020; Vol. 100, p 853-958.
- (12) Neeve, E. C.; Geier, S. J.; Mkhalid, I. A. I.; Westcott, S. A.; Marder, T. B. Diboron(4) Compounds: From Structural Curiosity to Synthetic Workhorse. *Chem. Rev.* **2016**, *116*, 9091-9161.
- (13) We note that while asymmetric hydrogenations have also been investigated in similar numbers to the transformations listed above, such reactions are outside the scope of this Perspective, which will principally focus on cross-coupling reactions.
- (14) Martin, R.; Buchwald, S. L. Palladium-Catalyzed Suzuki-Miyaura Cross-Coupling Reactions Employing Dialkylbiaryl Phosphine Ligands. *Acc. Chem. Res.* **2008**, *41*, 1461-1473.
- (15) Wu, H.; Qu, B.; Nguyen, T.; Lorenz, J. C.; Buono, F.; Haddad, N. Recent Advances in Non-Precious Metal Catalysis. *Org. Process Res. Dev.* **2022**, *26*, 2281-2310.

- (16) Bullock, R. M.; Chen, J. G.; Gagliardi, L.; Chirik, P. J.; Farha, O. K.; Hendon, C. H.; Jones, C. W.; Keith, J. A.; Klosin, J.; Minteer, S. D.; Morris, R. H.; Radosevich, A. T.; Rauchfuss, T. B.; Strotman, N. A.; Vojvodic, A.; Ward, T. R.; Yang, J. Y.; Surendranath, Y. Using nature's blueprint to expand catalysis with Earth-abundant metals. *Science* 2020, 369, eabc3183
- (17) Yaroshevsky, A. A. Abundances of chemical elements in the Earth's crust. Geochem. Int. 2006, 44, 48-55.
- (18) Nuss, P.; Eckelman, M. J. Life Cycle Assessment of Metals: A Scientific Synthesis. *PLOS ONE* **2014**, 9, e101298.
- (19) Similar trends are observed for other environmental factors such as cumulative energy demand (CED), terrestrial acidification, and freshwater eutrophication, indicating that the net environmental impact from precious metal usage is approximately 3 orders of magnitude higher compared to that of first row metals.
- (20) LI, J.; Albrecht, J.; Borovika, A.; Eastgate, M. D. Evolving Green Chemistry Metrics into Predictive Tools for Decision Making and Benchmarking Analytics. *ACS Sustainable Chem. Eng.* **2018**, *6*, 1121-1132.
- (21) (a) Yu, D.-G.; Li, B.-J.; Shi, Z.-J. Exploration of New C-O Electrophiles in Cross-Coupling Reactions. *Acc. Chem. Res.* **2010**, *43*, 1486-1495; (b) Qiu, Z.; Li, C.-J. Transformations of Less-Activated Phenols and Phenol Derivatives via C-O Cleavage. *Chem. Rev.* **2020**, *120*, 10454-10515.
- (22) Chan, A. Y.; Perry, I. B.; Bissonnette, N. B.; Buksh, B. F.; Edwards, G. A.; Frye, L. I.; Garry, O. L.; Lavagnino, M. N.; Li, B. X.; Liang, Y.; Mao, E.; Millet, A.; Oakley, J. V.; Reed, N. L.; Sakai, H. A.; Seath, C. P.; MacMillan, D. W. C. Metallaphotoredox: The Merger of Photoredox and Transition Metal Catalysis. *Chem. Rev.* **2022**, *122*, 1485-1542.
- (23) Malapit, C. A.; Prater, M. B.; Cabrera-Pardo, J. R.; Li, M.; Pham, T. D.; McFadden, T. P.; Blank, S.; Minteer, S. D. Advances on the Merger of Electrochemistry and Transition Metal Catalysis for Organic Synthesis. *Chem. Rev.* **2022**, *122*, 3180-3218.
- (24) Tay, N. E. S.; Lehnherr, D.; Rovis, T. Photons or Electrons? A Critical Comparison of Electrochemistry and Photoredox Catalysis for Organic Synthesis. *Chem. Rev.* **2022**, *122*, 2487-2649.
- (25) (a) Egorova, K. S.; Ananikov, V. P. Which Metals are Green for Catalysis? Comparison of the Toxicities of Ni, Cu, Fe, Pd, Pt, Rh, and Au Salts. *Angew. Chem. Int. Ed.* **2016**, *55*, 12150-12162; (b) Egorova, K. S.; Ananikov, V. P. Toxicity of Metal Compounds: Knowledge and Myths. *Organometallics* **2017**, *36*, 4071-4090.
- (26) <a href="https://database.ich.org/sites/default/files/Q3D-R2\_Guideline\_Step4\_2022\_0308.pdf">https://database.ich.org/sites/default/files/Q3D-R2\_Guideline\_Step4\_2022\_0308.pdf</a> (accessed October 2022)
- (27) Registration, Evaluation, Authorisation and Restriction of Chemicals.
- https://echa.europa.eu/regulations/reach/understanding-reach (accessed November 2022)
- (28) <a href="https://echa.europa.eu/substances-restricted-under-reach">https://echa.europa.eu/substances-restricted-under-reach</a> (accessed November 2022)
- (29) https://echa.europa.eu/recommendations-for-inclusion-in-the-authorisation-list (accessed November 2022)
- (30) Garrett Christine, E.; Prasad, K. The Art of Meeting Palladium Specifications in Active Pharmaceutical Ingredients Produced by Pd-Catalyzed Reactions. *Adv. Synth. Catal.* **2004**, *346*, 889-900.
- (31) (a) Tian, Q.; Cheng, Z.; Yajima, H. M.; Savage, S. J.; Green, K. L.; Humphries, T.; Reynolds, M. E.; Babu, S.; Gosselin, F.; Askin, D.; Kurimoto, I.; Hirata, N.; Iwasaki, M.; Shimasaki, Y.; Miki, T. A Practical Synthesis of a PI3K Inhibitor under Noncryogenic Conditions via Functionalization of a Lithium TriaryImagnesiate Intermediate. *Org. Process Res. Dev.* **2013**, *17*, 97-107; (b) Miki, T.; Shimasaki, Y.; Babu, S.; Cheng, Z.; Reynolds, M. E.; Tian, Q.; Sumitomo Chemical Co Ltd Genentech Inc: United States, 2009.
- (32) Chernyshev, V. M.; Ananikov, V. P. Nickel and Palladium Catalysis: Stronger Demand than Ever. ACS Catal. 2022, 12, 1180-1200.
- (33) Molander, G. A.; Cavalcanti, L. N.; García-García, C. Nickel-Catalyzed Borylation of Halides and Pseudohalides with Tetrahydroxydiboron [B<sub>2</sub>(OH)<sub>4</sub>]. *J. Org. Chem.* **2013**, *78*, 6427-6439.
- (34) (a) Watterson, S. H.; De Lucca, G. V.; Shi, Q.; Langevine, C. M.; Liu, Q.; Batt, D. G.; Beaudoin Bertrand, M.; Gong, H.; Dai, J.; Yip, S.; Li, P.; Sun, D.; Wu, D.-R.; Wang, C.; Zhang, Y.; Traeger, S. C.; Pattoli, M. A.; Skala, S.; Cheng, L.; Obermeier, M. T.; Vickery, R.; Discenza, L. N.; D'Arienzo, C. J.; Zhang, Y.; Heimrich, E.; Gillooly, K. M.; Taylor, T. L.; Pulicicchio, C.; McIntyre, K. W.; Galella, M. A.; Tebben, A. J.; Muckelbauer, J. K.; Chang, C.; Rampulla, R.; Mathur, A.; Salter-Cid, L.; Barrish, J. C.; Carter, P. H.; Fura, A.; Burke, J. R.; Tino, J. A. Discovery of 6-Fluoro-5-(*R*)-(3-(*S*)-(8-fluoro-1-methyl-2,4-dioxo-1,2-dihydroquinazolin-3(*4H*)-yl)-2-methylphenyl)-2-(*S*)-(2-hydroxypropan-2-yl)-2,3,4,9-tetrahydro-1*H*-carbazole-8-carboxamide (BMS-986142): A Reversible Inhibitor of Bruton's Tyrosine Kinase (BTK) Conformationally Constrained by Two Locked Atropisomers. *J. Med. Chem.* 2016, *59*, 9173-9200; (b) Beutner, G.; Carrasquillo, R.; Geng, P.; Hsiao, Y.; Huang, E. C.; Janey, J.; Katipally, K.; Kolotuchin, S.; La Porte, T.; Lee, A.; Lobben, P.; Lora-Gonzalez, F.; Mack, B.; Mudryk, B.; Qiu, Y.; Qian, X.; Ramirez, A.; Razler, T. M.; Rosner, T.; Shi, Z.; Simmons, E.; Stevens, J.; Wang, J.; Wei, C.; Wisniewski, S. R.; Zhu, Y. Adventures in Atropisomerism: Total Synthesis of a Complex Active Pharmaceutical Ingredient with Two Chirality Axes. *Org. Lett.* 2018, *20*, 3736-3740.
- (35) Coombs, J. R.; Green, R. A.; Roberts, F.; Simmons, E. M.; Stevens, J. M.; Wisniewski, S. R. Advances in Base-Metal Catalysis: Development of a Screening Platform for Nickel-Catalyzed Borylations of Aryl (Pseudo)halides with B<sub>2</sub>(OH)<sub>4</sub>. *Organometallics* **2019**, *38*, 157-166.
- (36) It should be noted that this estimated cost savings does not take into account any recycling of the spent palladium catalyst on production scale, which would lower the net cost of the palladium-catalyzed process and proportionally decrease the cost advantage of the nickel-catalyzed process.

- (37) Balog, A.; Lin, T.-a.; Maley, D.; Gullo-Brown, J.; Kandoussi, E. H.; Zeng, J.; Hunt, J. T. Preclinical Characterization of Linrodostat Mesylate, a Novel, Potent, and Selective Oral Indoleamine 2,3-Dioxygenase 1 Inhibitor. *Mol. Cancer Ther.* **2021**, *20*, 467-476.
- (38) Sonpavde, G.; Necchi, A.; Gupta, S.; Steinberg, G. D.; Gschwend, J. E.; Van Der Heijden, M. S.; Garzon, N.; Ibrahim, M.; Raybold, B.; Liaw, D.; Rutstein, M.; Galsky, M. D. ENERGIZE: a Phase III study of neoadjuvant chemotherapy alone or with nivolumab with/without linrodostat mesylate for muscle-invasive bladder cancer. *Future Oncol.* **2019**, *16*, 4359-4368.
- (39) Fraunhoffer, K. J.; DelMonte, A. J.; Beutner, G. L.; Bultman, M. S.; Camacho, K.; Cohen, B.; Dixon, D. D.; Fan, Y.; Fanfair, D.; Freitag, A. J.; Glace, A. W.; Gonzalez-Bobes, F.; Gujjar, M.; Haley, M. W.; Hickey, M. R.; Ho, J.; Iyer, V.; Maity, P.; Patel, S.; Rosso, V. W.; Schmidt, M. A.; Stevens, J. M.; Tan, Y.; Wilbert, C.; Young, I. S.; Yu, M. Rapid Development of a Commercial Process for Linrodostat, an Indoleamine 2,3-Dioxygenase (IDO) Inhibitor. *Org. Process Res. Dev.* **2019**, 23, 2482-2498.
- (40) Liu, X.-W.; Echavarren, J.; Zarate, C.; Martin, R. Ni-Catalyzed Borylation of Aryl Fluorides via C–F Cleavage. *J. Am. Chem. Soc.* **2015**, *137*, 12470-12473.
- (41) Cole, E.; Donnelly, D.; Wallace, M.; Tran, T.; Burrell, R.; Turley, W.; Allentoff, A.; Huang, A.; Balog, A.; Bonacorsi, S. Radiochemistry challenges and progression for incorporation of <sup>18</sup>F into a complex substituted 6-<sup>18</sup>F-fluoroquinoline BMS-986205 for IDO imaging. *J. Nucl. Med.* **2018**, *59*, 605.
- (42) (a) Donnelly, D. J.; Cole, E. L.; Burrell, R. C.; Turley, W. A.; Allentoff, A. J.; Wallace, M. A.; Balog, J. A.; Huang, A; Skinbjerg, M. Radioligands for imaging the IDO1 enzyme. WO 2018/017529, Bristol-Myers Squibb Company, USA . 49pp.; (b) Cole, E. L. et al, manuscript in preparation; (c) unpublished work, Bristol Myers Squibb, 2016.
- (43) Stevens, J. M.; Li, J.; Simmons, E. M.; Wisniewski, S. R.; DiSomma, S.; Fraunhoffer, K. J.; Geng, P.; Hao, B.; Jackson, E. W. Advancing Base Metal Catalysis through Data Science: Insight and Predictive Models for Ni-Catalyzed Borylation through Supervised Machine Learning. *Organometallics* **2022**, *41*, 1847-1864.
- (44) Gensch, T.; dos Passos Gomes, G.; Friederich, P.; Peters, E.; Gaudin, T.; Pollice, R.; Jorner, K.; Nigam, A.; Lindner-D'Addario, M.; Sigman, M. S.; Aspuru-Guzik, A. A Comprehensive Discovery Platform for Organophosphorus Ligands for Catalysis. *J. Am. Chem. Soc.* **2022**, *144*, 1205-1217.
- (45) Joannou, M. V.; Sarjeant, A. A.; Wisniewski, S. R. Diboron-Promoted Reduction of Ni(II) Salts: Precatalyst Activation Studies Relevant to Ni-Catalyzed Borylation Reactions. *Organometallics* **2021**, *40*, 2691-2700.
- (46) Baranwal, B. P.; Mehrotra, R. C. Synthesis and characterization of some alkoxide derivatives of nickel(II). *Aust. J. Chem.* **1980**, *33*, 37-43.
- (47) Wei, C. S.; Davies, G. H. M.; Soltani, O.; Albrecht, J.; Gao, Q.; Pathirana, C.; Hsiao, Y.; Tummala, S.; Eastgate, M. D. The Impact of Palladium(II) Reduction Pathways on the Structure and Activity of Palladium(0) Catalysts. *Angew. Chem. Int. Ed.* **2013**, *52*, 5822-5826.
- (48) (a) Molander, G. A.; Trice, S. L. J.; Dreher, S. D. Palladium-Catalyzed, Direct Boronic Acid Synthesis from Aryl Chlorides: A Simplified Route to Diverse Boronate Ester Derivatives. *J. Am. Chem. Soc.* **2010**, *132*, 17701-17703; (b) Molander, G. A.; Trice, S. L. J.; Kennedy, S. M. Scope of the Two-Step, One-Pot Palladium-Catalyzed Borylation/Suzuki Cross-Coupling Reaction Utilizing Bis-Boronic Acid. *J. Org. Chem.* **2012**, *77*, 8678-8688.
- (49) Smith, M. J.; Lawler, M. J.; Kopp, N.; McLeod, D. D.; Davulcu, A. H.; Lin, D.; Katipally, K.; Sfouggatakis, C. Development of a Concise Multikilogram Synthesis of LPA-1 Antagonist BMS-986020 via a Tandem Borylation—Suzuki Procedure. *Org. Process Res. Dev.* **2017**, *21*, 1859-1863.
- (50) Wilson, D. A.; Wilson, C. J.; Rosen, B. M.; Percec, V. Two-Step, One-Pot Ni-Catalyzed Neopentylglycolborylation and Complementary Pd/Ni-Catalyzed Cross-Coupling with Aryl Halides, Mesylates, and Tosylates. *Org. Lett.* **2008**, *10*, 4879-4882.
- (51) Munteanu, C.; Spiller, T. E.; Qiu, J.; DelMonte, A. J.; Wisniewski, S. R.; Simmons, E. M.; Frantz, D. E. Pd-and Ni-Based Systems for the Catalytic Borylation of Aryl (Pseudo)halides with B<sub>2</sub>(OH)<sub>4</sub>. *J. Org. Chem.* **2020**, *85*, 10334-10349.
- (52) Gurung, S. R.; Mitchell, C.; Huang, J.; Jonas, M.; Strawser, J. D.; Daia, E.; Hardy, A.; O'Brien, E.; Hicks, F.; Papageorgiou, C. D. Development and Scale-up of an Efficient Miyaura Borylation Process Using Tetrahydroxydiboron. *Org. Process Res. Dev.* **2017**, *21*, 65-74.
- (53) Merritt, J. M.; Borkar, I.; Buser, J. Y.; Brewer, A. C.; Campos, O.; Fleming, J.; Hansen, C.; Humenik, A.; Jeffery, S.; Kokitkar, P. B.; Kolis, S. P.; Forst, M. B.; Lambertus, G. R.; Martinelli, J. R.; McCartan, C.; Moursy, H.; Murphy, D.; Murray, M. M.; O'Donnell, K.; O'Sullivan, R.; Richardson, G. A.; Xia, H. Hydrogen Evolution from Telescoped Miyaura Borylation and Suzuki Couplings Utilizing Diboron Reagents: Process Safety and Hazard Considerations. *Org. Process Res. Dev.* **2022**, *26*, 773-784.
- (54) Palani, V.; Perea, M. A.; Sarpong, R. Site-Selective Cross-Coupling of Polyhalogenated Arenes and Heteroarenes with Identical Halogen Groups. *Chem. Rev.* **2022**, *122*, 10126-10169.
- (55) Percec, V.; Bae, J.-Y.; Hill, D. H. Aryl Mesylates in Metal Catalyzed Homocoupling and Cross-Coupling Reactions. 2. Suzuki-Type Nickel-Catalyzed Cross-Coupling of Aryl Arenesulfonates and Aryl Mesylates with Arylboronic Acids. *J. Org. Chem.* **1995**, *60*, 1060-1065.
- (56) Kobayashi, Y.; Mizojiri, R. Nickel-catalyzed coupling reaction of lithium organoborates and aryl mesylates possessing an electron withdrawing group. *Tetrahedron Lett.* **1996**, *37*, 8531-8534.

- (57) (a) Saito, S.; Sakai, M.; Miyaura, N. A synthesis of biaryls via nickel(0)-catalyzed cross-coupling reaction of chloroarenes with phenylboronic acids. *Tetrahedron Lett.* **1996**, *37*, 2993-2996; (b) Saito, S.; Oh-tani, S.; Miyaura, N. Synthesis of Biaryls via a Nickel(0)-Catalyzed Cross-Coupling Reaction of Chloroarenes with Arylboronic Acids. *J. Org. Chem.* **1997**, *62*, 8024-8030.
- (58) Indolese, A. F. Suzuki-type coupling of chloroarenes with arylboronic acids catalysed by nickel complexes. *Tetrahedron Lett.* **1997**, *38*, 3513-3516.
- (59) Inada, K.; Miyaura, N. Synthesis of Biaryls via Cross-Coupling Reaction of Arylboronic Acids with Aryl Chlorides Catalyzed by NiCl<sub>2</sub>/Triphenylphosphine Complexes. *Tetrahedron* **2000**, *56*, 8657-8660.
- (60) Hazari, N.; Melvin, P. R.; Beromi, M. M. Well-defined nickel and palladium precatalysts for cross-coupling. *Nat. Rev. Chem.* **2017**, *1*, 0025.
- (61) (a) Fan, X.-H.; Yang, L.-M. Room-Temperature Nickel-Catalysed Suzuki–Miyaura Reactions of Aryl Sulfonates/Halides with Arylboronic Acids. *Eur. J. Org. Chem.* **2011**, 2011, 1467-1471; (b) Ge, S.; Hartwig, J. F. Highly Reactive, Single-Component Nickel Catalyst Precursor for Suzuki–Miyuara Cross-Coupling of Heteroaryl Boronic Acids with Heteroaryl Halides. *Angew. Chem. Int. Ed.* **2012**, *51*, 12837-12841; (c) Jezorek, R. L.; Zhang, N.; Leowanawat, P.; Bunner, M. H.; Gutsche, N.; Pesti, A. K. R.; Olsen, J. T.; Percec, V. Air-Stable Nickel Precatalysts for Fast and Quantitative Cross-Coupling of Aryl Sulfamates with Aryl Neopentylglycolboronates at Room Temperature. *Org. Lett.* **2014**, *16*, 6326-6329.
- (62) For a recent example of a Ni-catalyzed Suzuki–Miyaura coupling that is tolerant of a large amount of water, see: Haibach, M. C.; Ickes, A. R.; Tcyrulnikov, S.; Shekhar, S.; Monfette, S.; Swiatowiec, R.; Kotecki, B. J.; Wang, J.; Wall, A. L.; Henry, R. F.; Hansen, E. C. Enabling Suzuki–Miyaura coupling of Lewis-basic arylboronic esters with a nonprecious metal catalyst. *Chem. Sci.* **2022**, *13*, 12906-12912.
- (63) Goldfogel, M. J.; Guo, X.; Meléndez Matos, J. L.; Gurak, J. A.; Joannou, M. V.; Moffat, W. B.; Simmons, E. M.; Wisniewski, S. R. Advancing Base-Metal Catalysis: Development of a Screening Method for Nickel-Catalyzed Suzuki–Miyaura Reactions of Pharmaceutically Relevant Heterocycles. *Org. Process Res. Dev.* **2022**, *26*, 785-794.
- (64) Analysis of the isolated solid for residual metal by X-ray fluorescence (XRF) indicated the presence of 4.1 ppm Ni. For a discussion on the application of XRF using field-portable instruments for metals analysis in pharmaceutical process development, see ref. 65.
- (65) Lewen, N.; Soumeillant, M.; Qiu, J.; Selekman, J.; Wood, S.; Zhu, K. Use of a Field-Portable XRF Instrument To Facilitate Metal Catalyst Scavenger Screening. *Org. Process Res. Dev.* **2015**, *19*, 2039-2044.
- (66) Lennox, A. J. J.; Lloyd-Jones, G. C. Organotrifluoroborate Hydrolysis: Boronic Acid Release Mechanism and an Acid–Base Paradox in Cross-Coupling. *J. Am. Chem. Soc.* **2012**, *134*, 7431-7441.
- (67) (a) Cooper, A. K.; Leonard, D. K.; Bajo, S.; Burton, P. M.; Nelson, D. J. Aldehydes and ketones influence reactivity and selectivity in nickel-catalysed Suzuki–Miyaura reactions. *Chem. Sci.* **2020**, *11*, 1905-1911; (b) Zell, D.; Kingston, C.; Jermaks, J.; Smith, S. R.; Seeger, N.; Wassmer, J.; Sirois, L. E.; Han, C.; Zhang, H.; Sigman, M. S.; Gosselin, F. Stereoconvergent and -divergent Synthesis of Tetrasubstituted Alkenes by Nickel-Catalyzed Cross-Couplings. *J. Am. Chem. Soc.* **2021**, *143*, 19078-19090.
- (68) Payard, P.-A.; Perego, L. A.; Ciofini, I.; Grimaud, L. Taming Nickel-Catalyzed Suzuki-Miyaura Coupling: A Mechanistic Focus on Boron-to-Nickel Transmetalation. *ACS Catal.* **2018**, *8*, 4812-4823.
- (69) Guo, X.; Dang, H.; Wisniewski, S. R.; Simmons, E. M. Nickel-Catalyzed Suzuki–Miyaura Cross-Coupling Facilitated by a Weak Amine Base with Water as a Cosolvent. *Organometallics* **2022**, *41*, 1269-1274.
- (70) Sawatzky, R. S.; Stradiotto, M. (DPEPhos)Ni(mesityl)Br: An Air-Stable Pre-Catalyst for Challenging Suzuki–Miyaura Cross-Couplings Leading to Unsymmetrical Biheteroaryls. *Synlett* **2018**, *29*, 799-804.
- (71) Simmons, E. M.; Mudryk, B.; Lee, A. G.; Qiu, Y.; Razler, T. M.; Hsiao, Y. Development of a Kilogram-Scale Process for the Enantioselective Synthesis of 3-Isopropenyl-cyclohexan-1-one via Rh/DTBM-SEGPHOS-Catalyzed Asymmetric Hayashi Addition Enabled by 1,3-Diol Additives. *Org. Process Res. Dev.* **2017**, *21*, 1659-1667.
- (72) Yang, Q.; Zhao, Y.; Ma, D. Cu-Mediated Ullmann-Type Cross-Coupling and Industrial Applications in Route Design, Process Development, and Scale-up of Pharmaceutical and Agrochemical Processes. *Org. Process Res. Dev.* **2022**, *26*, 1690-1750.
- (73) (a) Meyers, C.; Maes, B. U. W.; Loones, K. T. J.; Bal, G.; Lemière, G. L. F.; Dommisse, R. A. Study of a New Rate Increasing "Base Effect" in the Palladium-Catalyzed Amination of Aryl Iodides. *J. Org. Chem.* **2004**, *69*, 6010-6017; (b) Caygill, G.; Zanfir, M.; Gavriilidis, A. Scalable Reactor Design for Pharmaceuticals and Fine Chemicals Production. 1: Potential Scale-up Obstacles. *Org. Process Res. Dev.* **2006**, *10*, 539-552.
- (74) Lavoie, C. M.; Stradiotto, M. Bisphosphines: A Prominent Ancillary Ligand Class for Application in Nickel-Catalyzed C–N Cross-Coupling. *ACS Catal.* **2018**, *8*, 7228-7250.
- (75) Beutner, G. L.; Coombs, J. R.; Green, R. A.; Inankur, B.; Lin, D.; Qiu, J.; Roberts, F.; Simmons, E. M.; Wisniewski, S. R. Palladium-Catalyzed Amidation and Amination of (Hetero)aryl Chlorides under Homogeneous Conditions Enabled by a Soluble DBU/NaTFA Dual-Base System. *Org. Process Res. Dev.* **2019**, *23*, 1529-1537.
- (76) (a) Lundrigan, T.; Tassone, J. P.; Stradiotto, M. Nickel-Catalyzed *N*-Arylation of Amides with (Hetero)aryl Electrophiles by Using a DBU/NaTFA Dual-Base System. *Synlett* **2021**, *32*, 1665-1669; (b) McGuire, R. T.; Lundrigan, T.; MacMillan, J. W. M.; Robertson, K. N.; Yadav, A. A.; Stradiotto, M. Mapping Dual-Base-Enabled Nickel-Catalyzed Aryl Amidations: Application in the Synthesis of 4-Quinolones. *Angew. Chem. Int. Ed.* **2022**, *61*, e202200352.

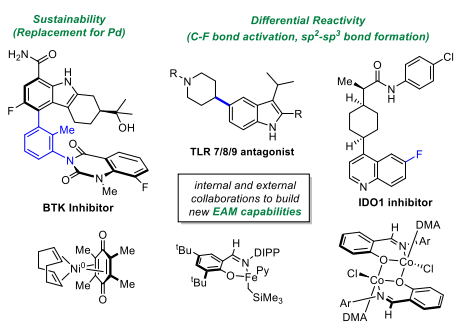
- (77) McGuire, R. T.; Yadav, A. A.; Stradiotto, M. Nickel-Catalyzed N-Arylation of Fluoroalkylamines. *Angew. Chem. Int. Ed.* **2021**, *60*, 4080-4084.
- (78) (a) Ullmann, F. Ueber eine neue Bildungsweise von Diphenylaminderivaten. *Ber. Dtsch. Chem. Ges.* **1903**, 36, 2382-2384; (b) Ullmann, F.; Sponagel, P. Ueber die Phenylirung von Phenolen. *Ber. Dtsch. Chem. Ges.* **1905**, 38, 2211-2212; (c) Goldberg, I. Ueber Phenylirungen bei Gegenwart von Kupfer als Katalysator. *Ber. Dtsch. Chem. Ges.* **1906**, 39, 1691-1692.
- (79) For pioneering reports on the development of versatile, air-stable Ni(II) precatalysts see: (a) Standley, E. A.; Smith, S. J.; Müller, P.; Jamison, T. F. A Broadly Applicable Strategy for Entry into Homogeneous Nickel(0) Catalysts from Air-Stable Nickel(II) Complexes. *Organometallics* **2014**, *33*, 2012-2018; (b) Magano, J.; Monfette, S. Development of an Air-Stable, Broadly Applicable Nickel Source for Nickel-Catalyzed Cross-Coupling. *ACS Catal.* **2015**, *5*, 3120-3123; (c) Shields, J. D.; Gray, E. E.; Doyle, A. G. A Modular, Air-Stable Nickel Precatalyst. *Org. Lett.* **2015**, *17*, 2166-2169.
- (80) (a) Zhuang, Z.; Yu, C.-B.; Chen, G.; Wu, Q.-F.; Hsiao, Y.; Joe, C. L.; Qiao, J. X.; Poss, M. A.; Yu, J.-Q. Ligand-Enabled  $\beta$ -C(sp³)–H Olefination of Free Carboxylic Acids. *J. Am. Chem. Soc.* **2018**, *140*, 10363-10367; (b) Sheng, T.; Zhuang, Z.; Wang, Z.; Hu, L.; Herron, A. N.; Qiao, J. X.; Yu, J.-Q. One-Step Synthesis of  $\beta$ -Alkylidene-γ-lactones via Ligand-Enabled  $\beta$ -Pohydrogenation of Aliphatic Acids. *J. Am. Chem. Soc.* **2022**, *144*, 12924-12933; (c) Zhuang, Z.; Liu, S.; Cheng, J.-T.; Yeung, K.-S.; Qiao, J. X.; Meanwell, N. A.; Yu, J.-Q. Ligand-Enabled  $\beta$ -C(sp³)–H Lactamization of Tosyl-Protected Aliphatic Amides Using a Practical Oxidant. *Angew. Chem. Int. Ed.* **2022**, *61*, e202207354.
- (81) Hao, W.; Joe, C. L.; Darù, A.; Ayers, S.; Ramirez, A.; Sandhu, B.; Daley, R. A.; Chen, J. S.; Schmidt, M. A.; Blackmond, D. G. Kinetic and Thermodynamic Considerations in the Rh-Catalyzed Enantioselective Hydrogenation of 2-Pyridyl-Substituted Alkenes. *ACS Catal.* **2022**, *12*, 5961-5969.
- (82) Hao, W.; Joe, C. L.; Ayers, S.; Darù, A.; Daley, R. A.; Domanski, M.; Chen, J. S.; Schmidt, M. A.; Blackmond, D. G. Ru-Catalyzed Enantioselective Hydrogenation of 2-Pyridyl-Substituted Alkenes and Substrate-Mediated H/D Exchange. *ACS Catal.* **2022**, *12*, 1150-1160.
- (83) Ji, Y.; Plata, Ř. E.; Regens, C. S.; Hay, M.; Schmidt, M.; Razler, T.; Qiu, Y.; Geng, P.; Hsiao, Y.; Rosner, T.; Eastgate, M. D.; Blackmond, D. G. Mono-Oxidation of Bidentate Bis-phosphines in Catalyst Activation: Kinetic and Mechanistic Studies of a Pd/Xantphos-Catalyzed C–H Functionalization. *J. Am. Chem. Soc.* **2015**, *137*, 13272-13281
- (84) Schultz, D.; Campeau, L.-C. Harder, better, faster. Nat. Chem. 2020, 12, 661-664.
- (85) Wethman, R.; Derosa, J.; Tran, V. T.; Kang, T.; Apolinar, O.; Abraham, A.; Kleinmans, R.; Wisniewski, S. R.; Coombs, J. R.; Engle, K. M. An Under-Appreciated Source of Reproducibility Issues in Cross-Coupling: Solid-State Decomposition of Primary Sodium Alkoxides in Air. *ACS Catal.* **2021**, *11*, 502-508.
- (86) Wender, P. A.; Smith, T. E.; Duong, H. A.; Louie, J.; Standley, E. A.; Tasker, S. Z. In *Encyclopedia of Reagents for Organic Synthesis*; John Wiley & Sons, Ltd: 2015.
- (87) Beutner, G. L.; Hsiao, Y.; Razler, T.; Simmons, E. M.; Wertjes, W. Nickel-Catalyzed Synthesis of Quinazolinediones. *Org. Lett.* **2017**, *19*, 1052-1055.
- (88) (a) Yoshino, Y.; Kurahashi, T.; Matsubara, S. Nickel-Catalyzed Decarboxylative Carboamination of Alkynes with Isatoic Anhydrides. *J. Am. Chem. Soc.* **2009**, *131*, 7494-7495; (b) Sun, M.; Ma, Y.-N.; Li, Y.-M.; Tian, Q.-P.; Yang, S.-D. Nickel-catalyzed decarboxylative cycloaddition of isatoic anhydrides with alkenes. *Tetrahedron Lett.* **2013**, *54*, 5091-5095; (c) Nakai, K.; Kurahashi, T.; Matsubara, S. Nickel-catalyzed Decarbonylative and Decarboxylative Cycloaddition of Isatoic Anhydrides with Alkynes. *Chem. Lett.* **2013**, *42*, 1238-1240.
- (89) (a) Tanaka, K.; Wada, A.; Noguchi, K. Rhodium-Catalyzed Chemo-, Regio-, and Enantioselective [2 + 2 + 2] Cycloaddition of Alkynes with Isocyanates. *Org. Lett.* **2005**, *7*, 4737-4739; (b) Tanaka, K.; Takahashi, Y.; Suda, T.; Hirano, M. Synthesis of Enantioenriched *N*-Aryl-2-pyridones with Chiral C–N Axes by Rhodium-Catalyzed [2+2+2] Cycloaddition of Alkynes with Isocyanates. *Synlett* **2008**, *2008*, 1724-1728.
- (90) Dander, J. E.; Weires, N. A.; Garg, N. K. Benchtop Delivery of Ni(cod)<sub>2</sub> using Paraffin Capsules. *Org. Lett.* **2016**, *18*, 3934-3936.
- (91) Sather, A. C.; Lee, H. G.; Colombe, J. R.; Zhang, A.; Buchwald, S. L. Dosage delivery of sensitive reagents enables glove-box-free synthesis. *Nature* **2015**, *524*, 208-211.
- (92) Wilke, G. Contributions to Organo-Nickel Chemistry. Angew. Chem. Int. Ed. Engl. 1988, 27, 185-206.
- (93) (a) Nattmann, L.; Saeb, R.; Nöthling, N.; Cornella, J. An air-stable binary Ni(0)–olefin catalyst. *Nature Catalysis* **2020**, *3*, 6-13; (b) Nattmann, L.; Cornella, J. Ni(<sup>4-tBu</sup>stb)<sub>3</sub>: A Robust 16-Electron Ni(0) Olefin Complex for Catalysis. *Organometallics* **2020**, *39*, 3295-3300.
- (94) Saeb, R.; Cornella, J. STREM Chemiker. 2021, vol. XXXII, No 1, 1-14.
- (95) Buech, H. M.; Binger, P.; Krueger, C. Preparation, structure, and ligand substitution reactions of (cycloocta-1,5-diene)[methyl trans-β-(phenylsulfonyl)acrylate]nickel. *Organometallics* **1984**, *3*, 1504-1509.
- (96) Schrauzer, G. N.; Thyret, H. Neuartige "Sandwich"-Verbindungen des Nickel(0). Zur Kenntnis von Durodiinon-Nickel(0)-Komplexen mit cyclischen Dienen. *Z. Naturforsch. B* **1962**, *17*, 73-76.
- (97) Tran, V. T.; Li, Z.-Q.; Apolinar, O.; Derosa, J.; Joannou, M. V.; Wisniewski, S. R.; Eastgate, M. D.; Engle, K. M. Ni(COD)(DQ): An Air-Stable 18-Electron Nickel(0)–Olefin Precatalyst. *Angew. Chem. Int. Ed.* **2020**, *59*, 7409-7413.

- (98) (a) Li, Y.; Shao, Q.; He, H.; Zhu, C.; Xue, X.-S.; Xie, J. Highly selective synthesis of all-carbon tetrasubstituted alkenes by deoxygenative alkenylation of carboxylic acids. *Nat. Commun.* **2022**, *13*, 10; (b) Roediger, S.; Leutenegger, S. U.; Morandi, B. Nickel-catalysed diversification of phosphine ligands by formal substitution at phosphorus. *Chem. Sci.* **2022**, *13*, 7914-7919; (c) You, T.; Li, J. Ni(cod)(duroquinone)-Catalyzed C–N Cross-Coupling for the Synthesis of N,N-Diarylsulfonamides. *Org. Lett.* **2022**, *24*, 6642-6646.
- (99) Reilly, S. W.; Lam, Y.-h.; Ren, S.; Strotman, N. A. Late-Stage Carbon Isotope Exchange of Aryl Nitriles through Ni-Catalyzed C–CN Bond Activation. *J. Am. Chem. Soc.* **2021**, *143*, 4817-4823.
- (100) Tran, V. T.; Kim, N.; Rubel, C. Z.; Wu, X.; Kang, T.; Jankins, T. C.; Li, Z.-Q.; Joannou, M. V.; Ayers, S.; Gembicky, M.; Bailey, J.; Sturgell, E. J.; Sanchez, B. B.; Chen, J. S.; Lin, S.; Eastgate, M. D.; Wisniewski, S. R.; Engle, K. M. Structurally Diverse Bench-Stable Nickel(0) Pre-Catalysts: A Practical Toolkit for In Situ Ligation Protocols. *Angew. Chem. Int. Ed.* **2023**, *62*, e202211794.
- (101) Derosa, J.; Kleinmans, R.; Tran, V. T.; Karunananda, M. K.; Wisniewski, S. R.; Eastgate, M. D.; Engle, K. M. Nickel-Catalyzed 1,2-Diarylation of Simple Alkenyl Amides. *J. Am. Chem. Soc.* **2018**, *140*, 17878-17883.
- (102) Derosa, J.; Kang, T.; Tran, V. T.; Wisniewski, S. R.; Karunananda, M. K.; Jankins, T. C.; Xu, K. L.; Engle, K. M. Nickel-Catalyzed 1,2-Diarylation of Alkenyl Carboxylates: A Gateway to 1,2,3-Trifunctionalized Building Blocks. *Angew. Chem. Int. Ed.* **2020**, *59*, 1201-1205.
- (103) Kleinmans, R.; Apolinar, O.; Derosa, J.; Karunananda, M. K.; Li, Z.-Q.; Tran, V. T.; Wisniewski, S. R.; Engle, K. M. Ni-Catalyzed 1,2-Diarylation of Alkenyl Ketones: A Comparative Study of Carbonyl-Directed Reaction Systems. *Org. Lett.* **2021**, *23*, 5311-5316.
- (104) Li, Z.-Q.; He, W.-J.; Ni, H.-Q.; Engle, K. M. Directed, nickel-catalyzed 1,2-alkylsulfenylation of alkenyl carbonyl compounds. *Chem. Sci.* **2022**, *13*, 6567-6572.
- (105) While toxicity and safety data on the Ni(0)(COD)(L) sources prepared in collaboration with Prof. Engle's group have not yet been collected, this information would be important prior to any large-scale applications using these species.
- (106) Thapa, S.; Shrestha, B.; Gurung, S. K.; Giri, R. Copper-catalysed cross-coupling: an untapped potential. *Org. Biomol. Chem.* **2015**, *13*, 4816-4827.
- (107) (a) Li, J.-H.; Li, J.-L.; Wang, D.-P.; Pi, S.-F.; Xie, Y.-X.; Zhang, M.-B.; Hu, X.-C. Cul-Catalyzed Suzuki-Miyaura and Sonogashira Cross-Coupling Reactions Using DABCO as Ligand. *J. Org. Chem.* **2007**, *72*, 2053-2057; (b) Gurung, S. K.; Thapa, S.; Kafle, A.; Dickie, D. A.; Giri, R. Copper-Catalyzed Suzuki-Miyaura Coupling of Arylboronate Esters: Transmetalation with (PN)CuF and Identification of Intermediates. *Org. Lett.* **2014**, *16*, 1264-1267; (c) Zhou, Y.; You, W.; Smith, K. B.; Brown, M. K. Copper-Catalyzed Cross-Coupling of Boronic Esters with Aryl lodides and Application to the Carboboration of Alkynes and Allenes. *Angew. Chem. Int. Ed.* **2014**, *53*, 3475-3479; (d) Gurung, S. K.; Thapa, S.; Shrestha, B.; Giri, R. Copper-catalysed cross-couplings of arylboronate esters with aryl and heteroaryl iodides and bromides. *Org. Chem. Front.* **2015**, *2*, 649-653; (e) Bergmann, A. M.; Oldham, A. M.; You, W.; Brown, M. K. Copper-catalyzed cross-coupling of aryl-, primary alkyl-, and secondary alkylboranes with heteroaryl bromides. *Chem. Commun.* **2018**, *54*, 5381-5384.
- (108) (a) Adams, R. W.; Bishop, E.; Martin, R. L.; Winter, G. Magnetism, electronic spectra, and structure of transition metal alkoxides. I. methoxides and ethoxides of chromium(II), manganese(II), Iron(II), cobalt(II), nickel(II), copper(II), titanium(III), chromium(III), and iron(III). *Aust. J. Chem.* **1966**, *19*, 207-210; (b) Olmstead, M. M.; Power, P. P.; Sigel, G. Mononuclear cobalt(II) complexes having alkoxide and amide ligands: synthesis and x-ray crystal structures of [Co(Cl)(OC-t-Bu<sub>3</sub>)<sub>2</sub>•Li(THF)<sub>3</sub>], [Li(THF)<sub>4-5</sub>][Co{N(SiMe<sub>3</sub>)<sub>2</sub>}(OC-t-Bu<sub>3</sub>)<sub>2</sub>], and [Li{Co(N(SiMe<sub>3</sub>)<sub>2</sub>)(OC-t-Bu<sub>3</sub>)<sub>2</sub>]. *Inorg. Chem.* **1986**, *25*, 1027-1033; (c) Taft, K. L.; Caneschi, A.; Pence, L. E.; Delfs, C. D.; Papaefthymiou, G. C.; Lippard, S. J. Iron and manganese alkoxide cubes. *J. Am. Chem. Soc.* **1993**, *115*, 11753-11766; (d) Gun'ko, Yurii K.; Cristmann, U.; Kessler, Vadim G. Synthesis and Structure of the First FeII Heterometallic Alkoxide [(THF)NaFe(OtBu)<sub>3</sub>]<sub>2</sub> a Possible Precursor for New Materials. *Eur. J. Inorg. Chem.* **2002**, *2002*, 1029-1031; (e) Tailor, S. B.; Manzotti, M.; Smith, G. J.; Davis, S. A.; Bedford, R. B. Cobalt-Catalyzed Coupling of Aryl Chlorides with Aryl Boron Esters Activated by Alkoxides. *ACS Catal.* **2021**, *11*, 3856-3866.
- (109) Neely, J. M.; Bezdek, M. J.; Chirik, P. J. Insight into Transmetalation Enables Cobalt-Catalyzed Suzuki–Miyaura Cross Coupling. *ACS Cent. Sci.* **2016**, *2*, 935-942.
- (110) Duong, H. A.; Wu, W.; Teo, Y.-Y. Cobalt-Catalyzed Cross-Coupling Reactions of Arylboronic Esters and Aryl Halides. *Organometallics* **2017**, *36*, 4363-4366.
- (111) Peterson, P. O.; Rummelt, S. M.; Wile, B. M.; Stieber, S. C. E.; Zhong, H.; Chirik, P. J. Direct Observation of Transmetalation from a Neutral Boronate Ester to a Pyridine(diimine) Iron Alkoxide. *Organometallics* **2020**, *39*, 201-205.
- (112) Frisch, A. C.; Beller, M. Catalysts for Cross-Coupling Reactions with Non-activated Alkyl Halides. *Angew. Chem. Int. Ed.* **2005**, *44*, 674-688.
- (113) (a) Ishiyama, T.; Abe, S.; Miyaura, N.; Suzuki, A. Palladium-Catalyzed Alkyl-Alkyl Cross-Coupling Reaction of 9-Alkyl-9-BBN Derivatives with Iodoalkanes Possessing β-Hydrogens. *Chem. Lett.* **1992**, *21*, 691-694; (b) Netherton, M. R.; Fu, G. C. Suzuki Cross-Couplings of Alkyl Tosylates that Possess β Hydrogen Atoms: Synthetic and Mechanistic Studies. *Angew. Chem. Int. Ed.* **2002**, *41*, 3910-3912.

- (114) (a) Hu, X. Nickel-catalyzed cross coupling of non-activated alkyl halides: a mechanistic perspective. *Chem. Sci.* **2011**, 2, 1867-1886; (b) Han, F.-S. Transition-metal-catalyzed Suzuki-Miyaura cross-coupling reactions: a remarkable advance from palladium to nickel catalysts. *Chem. Soc. Rev.* **2013**, *42*, 5270-5298.
- (115) (a) Cornella, J.; Edwards, J. T.; Qin, T.; Kawamura, S.; Wang, J.; Pan, C.-M.; Gianatassio, R.; Schmidt, M.; Eastgate, M. D.; Baran, P. S. Practical Ni-Catalyzed Aryl–Alkyl Cross-Coupling of Secondary Redox-Active Esters. *J. Am. Chem. Soc.* **2016**, *138*, 2174-2177; (b) Wang, J.; Qin, T.; Chen, T.-G.; Wimmer, L.; Edwards, J. T.; Cornella, J.; Vokits, B.; Shaw, S. A.; Baran, P. S. Nickel-Catalyzed Cross-Coupling of Redox-Active Esters with Boronic Acids. *Angew. Chem. Int. Ed.* **2016**, *55*, 9676-9679; (c) Sandfort, F.; O'Neill, M. J.; Cornella, J.; Wimmer, L.; Baran, P. S. Alkyl–(Hetero)Aryl Bond Formation via Decarboxylative Cross-Coupling: A Systematic Analysis. *Angew. Chem. Int. Ed.* **2017**, *56*, 3319-3323; (d) Edwards, J. T.; Merchant, R. R.; McClymont, K. S.; Knouse, K. W.; Qin, T.; Malins, L. R.; Vokits, B.; Shaw, S. A.; Bao, D.-H.; Wei, F.-L.; Zhou, T.; Eastgate, M. D.; Baran, P. S. Decarboxylative alkenylation. *Nature* **2017**, *545*, 213-218.
- (116) Paik, A.; Paul, S.; Bhowmik, S.; Das, R.; Naveen, T.; Rana, S. Recent Advances in First-Row Transition-Metal-Mediated C-H Halogenation of (Hetero)arenes and Alkanes. *Asian Journal of Organic Chemistry* **2022**, *11*, e202200060
- (117) Liu, T.; Myers, M. C.; Yu, J.-Q. Copper-Catalyzed Bromination of C(sp³)–H Bonds Distal to Functional Groups. *Angew. Chem. Int. Ed.* **2017**, *56*, 306-309.
- (118) (a) Lovering, F.; Bikker, J.; Humblet, C. Escape from Flatland: Increasing Saturation as an Approach to Improving Clinical Success. *J. Med. Chem.* **2009**, *52*, 6752-6756; (b) Lovering, F. Escape from Flatland 2: complexity and promiscuity. *Med. Chem. Commun.* **2013**, *4*, 515-519.
- (119) Ishikawa, M.; Hashimoto, Y. Improvement in Aqueous Solubility in Small Molecule Drug Discovery Programs by Disruption of Molecular Planarity and Symmetry. *J. Med. Chem.* **2011**, *54*, 1539-1554.
- (120) Mussari, C. P.; Dodd, D. S.; Sreekantha, R. K.; Pasunoori, L.; Wan, H.; Posy, S. L.; Critton, D.; Ruepp, S.; Subramanian, M.; Watson, A.; Davies, P.; Schieven, G. L.; Salter-Cid, L. M.; Srivastava, R.; Tagore, D. M.; Dudhgaonkar, S.; Poss, M. A.; Carter, P. H.; Dyckman, A. J. Discovery of Potent and Orally Bioavailable Small Molecule Antagonists of Toll-like Receptors 7/8/9 (TLR7/8/9). *ACS Med. Chem. Lett.* **2020**, *11*, 1751-1758.
- (121) Beutner, G. L.; Simmons, E. M.; Ayers, S.; Bemis, C. Y.; Goldfogel, M. J.; Joe, C. L.; Marshall, J.; Wisniewski, S. R. A Process Chemistry Benchmark for sp<sup>2</sup>–sp<sup>3</sup> Cross Couplings. *J. Org. Chem.* **2021**, *86*, 10380-10396.
- (122) Zhou, J.; Fu, G. C. Suzuki Cross-Couplings of Unactivated Secondary Alkyl Bromides and Iodides. *J. Am. Chem. Soc.* **2004**, *126*, 1340-1341.
- (123) (a) Everson, D. A.; Jones, B. A.; Weix, D. J. Replacing Conventional Carbon Nucleophiles with Electrophiles: Nickel-Catalyzed Reductive Alkylation of Aryl Bromides and Chlorides. *J. Am. Chem. Soc.* **2012**, *134*, 6146-6159; (b) Molander, G. A.; Traister, K. M.; O'Neill, B. T. Reductive Cross-Coupling of Nonaromatic, Heterocyclic Bromides with Aryl and Heteroaryl Bromides. *J. Org. Chem.* **2014**, *79*, 5771-5780.
- (124) Molander, G. A.; Traister, K. M.; O'Neill, B. T. Engaging Nonaromatic, Heterocyclic Tosylates in Reductive Cross-Coupling with Aryl and Heteroaryl Bromides. *J. Org. Chem.* **2015**, *80*, 2907-2911.
- (125) Nimmagadda, S. K.; Korapati, S.; Dasgupta, D.; Malik, N. A.; Vinodini, A.; Gangu, A. S.; Kalidindi, S.; Maity, P.; Bondigela, S. S.; Venu, A.; Gallagher, W. P.; Aytar, S.; González-Bobes, F.; Vaidyanathan, R. Development and Execution of an Ni(II)-Catalyzed Reductive Cross-Coupling of Substituted 2-Chloropyridine and Ethyl 3-Chloropropanoate. *Org. Process Res. Dev.* **2020**, *24*, 1141-1148.
- (126) Charboneau, D. J.; Hazari, N.; Huang, H.; Uehling, M. R.; Zultanski, S. L. Homogeneous Organic Electron Donors in Nickel-Catalyzed Reductive Transformations. *J. Org. Chem.* **2022**, *87*, 7589-7609.
- (127) Perkins, R. J.; Pedro, D. J.; Hansen, E. C. Electrochemical Nickel Catalysis for Sp<sup>2</sup>-Sp<sup>3</sup> Cross-Electrophile Coupling Reactions of Unactivated Alkyl Halides. *Org. Lett.* **2017**, *19*, 3755-3758.
- (128) Zhang, P.; Le, C. C.; MacMillan, D. W. C. Silyl Radical Activation of Alkyl Halides in Metallaphotoredox Catalysis: A Unique Pathway for Cross-Electrophile Coupling. *J. Am. Chem. Soc.* **2016**, *138*, 8084-8087.
- (129) Zuo, Z.; Ahneman, D. T.; Chu, L.; Terrett, J. A.; Doyle, A. G.; MacMillan, D. W. C. Merging photoredox with nickel catalysis: Coupling of α-carboxyl sp³-carbons with aryl halides. *Science* **2014**, *345*, 437-440.
- (130) Cauley, A. N.; Ramirez, A.; Barhate, C. L.; Donnell, A. F.; Khandelwal, P.; Sezen-Edmonds, M.; Sherwood, T. C.; Sloane, J. L.; Cavallaro, C. L.; Simmons, E. M. Ni/Photoredox-Catalyzed C(sp²)–C(sp³) Cross-Coupling of Alkyl Pinacolboronates and (Hetero)Aryl Bromides. *Org. Lett.* **2022**, *24*, 5663-5668.
- (131) Speckmeier, E.; Fischer, T. G.; Zeitler, K. A Toolbox Approach To Construct Broadly Applicable Metal-Free Catalysts for Photoredox Chemistry: Deliberate Tuning of Redox Potentials and Importance of Halogens in Donor–Acceptor Cyanoarenes. *J. Am. Chem. Soc.* **2018**, *140*, 15353-15365.
- (132) Yang, C.-T.; Zhang, Z.-Q.; Liu, Y.-C.; Liu, L. Copper-Catalyzed Cross-Coupling Reaction of Organoboron Compounds with Primary Alkyl Halides and Pseudohalides. *Angew. Chem. Int. Ed.* **2011**, *50*, 3904-3907.
- (133) Taylor, R. D.; MacCoss, M.; Lawson, A. D. G. Rings in Drugs. J. Med. Chem. 2014, 57, 5845-5859.
- (134) (a) Vitaku, E.; Smith, D. T.; Njardarson, J. T. Analysis of the Structural Diversity, Substitution Patterns, and Frequency of Nitrogen Heterocycles among U.S. FDA Approved Pharmaceuticals. *J. Med. Chem.* **2014**, *57*, 10257-10274; (b) Goel, P.; Alam, O.; Naim, M. J.; Nawaz, F.; Iqbal, M.; Alam, M. I. Recent advancement of piperidine moiety in treatment of cancer- A review. *Eur. J. Med. Chem.* **2018**, *157*, 480-502.

- (135) Ludwig, J. R.; Simmons, E. M.; Wisniewski, S. R.; Chirik, P. J. Cobalt-Catalyzed C(sp<sup>2</sup>)–C(sp<sup>3</sup>) Suzuki–Miyaura Cross Coupling. *Org. Lett.* **2021**, *23*, 625-630.
- (136) Mills, L. R.; Gygi, D.; Ludwig, J. R.; Simmons, E. M.; Wisniewski, S. R.; Kim, J.; Chirik, P. J. Cobalt-Catalyzed C(sp²)–C(sp³) Suzuki–Miyaura Cross-Coupling Enabled by Well-Defined Precatalysts with L,X-Type Ligands. *ACS Catal.* **2022**, *12*, 1905-1918.
- (137) (a) Younkin, T. R.; Connor, E. F.; Henderson, J. I.; Friedrich, S. K.; Grubbs, R. H.; Bansleben, D. A. Neutral, Single-Component Nickel (II) Polyolefin Catalysts That Tolerate Heteroatoms. *Science* **2000**, *287*, 460-462; (b) Furuyama, R.; Saito, J.; Ishii, S.; Makio, H.; Mitani, M.; Tanaka, H.; Fujita, T. Fluorinated bis(phenoxy–imine) Ti complexes with MAO: Remarkable catalysts for living ethylene and syndioselective living propylene polymerization. *J. Organomet. Chem.* **2005**, *690*, 4398-4413; (c) Yuan, S.-F.; Yan, Y.; Solan, G. A.; Ma, Y.; Sun, W.-H. Recent advancements in *N*-ligated group 4 molecular catalysts for the (co)polymerization of ethylene. *Coord. Chem. Rev.* **2020**, *411*, 213254.
- (138) Bedford, R. B.; Hall, M. A.; Hodges, G. R.; Huwe, M.; Wilkinson, M. C. Simple mixed Fe–Zn catalysts for the Suzuki couplings of tetraarylborates with benzyl halides and 2-halopyridines. *Chem. Commun.* **2009**, 6430-6432.
- (139) (a) Hatakeyama, T.; Hashimoto, T.; Kondo, Y.; Fujiwara, Y.; Seike, H.; Takaya, H.; Tamada, Y.; Ono, T.; Nakamura, M. Iron-Catalyzed Suzuki-Miyaura Coupling of Alkyl Halides. *J. Am. Chem. Soc.* **2010**, *132*, 10674-10676; (b) Hashimoto, T.; Hatakeyama, T.; Nakamura, M. Stereospecific Cross-Coupling between Alkenylboronates and Alkyl Halides Catalyzed by Iron-Bisphosphine Complexes. *J. Org. Chem.* **2012**, *77*, 1168-1173.
- (140) Bedford, R. B., Brenner, P. B., Carter, E., Carvell, T. W., Cogswell, P. M., Gallagher, T., Harvey, J. N., Murphy, D. M., Neeve, E. C., Nunn, J., Pye, D. R. Expedient Iron-Catalyzed Coupling of Alkyl, Benzyl and Allyl Halides with Arylboronic Esters. *Chem. Eur. J.* **2014**, *20*, 7935-7938.
- (141) Rathman, T. L.; Schwindeman, J. A. Preparation, Properties, and Safe Handling of Commercial Organolithiums: Alkyllithiums, Lithium sec-Organoamides, and Lithium Alkoxides. *Org. Process Res. Dev.* **2014**, *18*, 1192-1210.
- (142) (a) Crockett, M. P.; Tyrol, C. C.; Wong, A. S.; Li, B.; Byers, J. A. Iron-Catalyzed Suzuki–Miyaura Cross-Coupling Reactions between Alkyl Halides and Unactivated Arylboronic Esters. *Org. Lett.* **2018**, *20*, 5233-5237; (b) Crockett, M. P.; Wong, A. S.; Li, B.; Byers, J. A. Rational Design of an Iron-Based Catalyst for Suzuki–Miyaura Cross-Couplings Involving Heteroaromatic Boronic Esters and Tertiary Alkyl Electrophiles. *Angew. Chem. Int. Ed.* **2020**, *59*, 5392-5397; (c) Tyrol, C. C.; Yone, N. S.; Gallin, C. F.; Byers, J. A. Iron-catalysed enantioconvergent Suzuki–Miyaura cross-coupling to afford enantioenriched 1,1-diarylalkanes. *Chem. Commun.* **2020**, *56*, 14661-14664; (d) Wong, A. S.; Zhang, B.; Li, B.; Neidig, M. L.; Byers, J. A. Air-Stable Iron-Based Precatalysts for Suzuki–Miyaura Cross-Coupling Reactions between Alkyl Halides and Aryl Boronic Esters. *Org. Process Res. Dev.* **2021**, *25*, 2461-2472.
- (143) Henderson, R. K.; Hill, A. P.; Redman, A. M.; Sneddon, H. F. Development of GSK's acid and base selection guides. *Green Chem.* **2015**, *17*, 945-949.
- (144) Peterson, P. O.; Joannou, M. V.; Simmons, E. M.; Wisniewski, S. R.; Kim, J.; Chirik, P. J. Iron-Catalyzed C(sp²)–C(sp³) Suzuki–Miyaura Cross-Coupling Using an Alkoxide Base. *ACS Catal.* **2023**, *13*, 2443-2448.
- (145) Trost, B. M. The Atom Economy—A Search for Synthetic Efficiency. Science 1991, 254, 1471-1477.
- (146) (a) Jimenez-Gonzalez, C.; Ponder, C. S.; Broxterman, Q. B.; Manley, J. B. Using the Right Green Yardstick: Why Process Mass Intensity Is Used in the Pharmaceutical Industry To Drive More Sustainable Processes. *Org. Process Res. Dev.* **2011**, *15*, 912-917; (b) Borovika, A.; Albrecht, J.; Li, J.; Wells, A. S.; Briddell, C.; Dillon, B. R.; Diorazio, L. J.; Gage, J. R.; Gallou, F.; Koenig, S. G.; Kopach, M. E.; Leahy, D. K.; Martinez, I.; Olbrich, M.; Piper, J. L.; Roschangar, F.; Sherer, E. C.; Eastgate, M. D. The PMI Predictor app to enable green-by-design chemical synthesis. *Nature Sustainability* **2019**, *2*, 1034-1040.
- (147) Li, J.; Eastgate, M. D. Making better decisions during synthetic route design: leveraging prediction to achieve greenness-by-design. *React. Chem. Eng.* **2019**, *4*, 1595-1607.
- (148) PMI could only be approximated as exact amounts of extraction solvents were not provided in the experimental details.
- (149) Vallée, F.; Kühn, F. E.; Korinth, V. A. In *Encyclopedia of Reagents for Organic Synthesis*; John Wiley & Sons, Ltd: 2013.
- (150) Leahy, D. K.; Simmons, E. M.; Hung, V.; Sweeney, J. T.; Fleming, W. F.; Miller, M. Design and evolution of the BMS process greenness scorecard. *Green Chem.* **2017**, *19*, 5163-5171.

# TOC graphic



Precatalyst and Reaction Development